The Meteoritical Society

Meteoritics & Planetary Science 42, Nr 3, 387–412 (2007)
Abstract available online at http://meteoritics.org

Noble gases in mineral separates from three shergottites: Shergotty, Zagami, and EETA79001

Susanne P. SCHWENZER*, Siegfried HERRMANN, Ratan K. MOHAPATRA†, and Ulrich OTT

Max-Planck-Institut für Chemie, J.-J. Becher Weg 27, D-55128 Mainz, Germany
†Present address: University of Ottawa, Department of Earth Sciences, Ottawa, Ontario K1N 6N5, Canada
*Corresponding author. E-mail: schwenze@mpch-mainz.mpg.de

(Received 02 June 2006; revision accepted 26 July 2006)

Abstract–This study provides a complete data set of all five noble gases for bulk samples and mineral separates from three Martian shergottites: Shergotty (bulk, pyroxene, maskelynite), Zagami (bulk, pyroxene, maskelynite), and Elephant Moraine (EET) A79001, lithology A (bulk, pyroxene). We also give a compilation of all noble gas and nitrogen studies performed on these meteorites. Our mean values for cosmic-ray exposure ages from ^{3}He, ^{21}Ne, and ^{38}Ar are 2.48 Myr for Shergotty, 2.73 Myr for Zagami, and 0.65 Myr for EETA79001 lith. A. Serious loss of radiogenic ^{4}He due to shock is observed. Cosmogenic neon results for bulk samples from 13 Martian meteorites (new data and literature data) are used in addition to the mineral separates of this study in a new approach to explore evidence of solar cosmic-ray effects. While a contribution of this low-energy irradiation is strongly indicated for all of the shergottites, spallation Ne in Chassigny, Allan Hills (ALH) 84001, and the nakhlites is fully explained by galactic cosmic-ray spallation. Implanted Martian atmospheric gases are present in all mineral separates and the thermal release indicates a near-surface siting. We derive an estimate for the ^{40}Ar/^{36}Ar ratio of the Martian interior component by subtracting from measured Ar in the (K-poor) pyroxenes the (small) radiogenic component as well as the implanted atmospheric component as indicated from ^{129}Xe* excesses. Unless compromised by the presence of additional components, a high ratio of ~2000 is indicated for Martian interior argon, similar to that in the Martian atmosphere. Since much lower ratios have been inferred for Chassigny and ALH 84001, the result may indicate spatial and/or temporal variations of ^{40}Ar/^{36}Ar in the Martian mantle.

INTRODUCTION

The SNC group of igneous meteorites was named after three "typical" samples of the group: Shergotty, Nakhla, and Chassigny. Long before the scientific community realized that the SNC meteorites are "exotic" with respect to some of their features compared to other meteorites (including other igneous meteorites), precise descriptions of single samples had been made, e.g., by Tschermak, who in the nineteenth century described the nature of the amorphous constituent maskelynite (Tschermak 1872, 1883). More than 100 years after Tschermak (1872) made Shergotty the "type locality" of maskelynite, Clayton and Mayeda (1983) found that the SNC meteorites lie on a fractionation line in oxygen isotopes displaced from those of Earth and eucrites. This reflects a distinct parent body different from Earth and the Moon, and the howardite, eucrite, and diogenite (HED) parent body, presumably asteroid 4 Vesta. Furthermore, compared to other meteorites and lunar samples, the SNC meteorites differ not only in oxygen isotopes, but also in several other characteristic chemical and isotopic features, e.g., implied oxygen fugacity (see McSween 1984, 1994, and 2002 for a review). In addition, not only does the group include more highly differentiated rock types like basalts, but these are also characterized by young crystallization ages (McSween 1984, 1994, 2002; Meyer 2003; Nyquist et al. 2001).

Already in 1966 Wänke considered the possibility of Moon and Mars being parent bodies of certain meteorites (Wänke 1966); however, starting around 1980, more and more authors seriously considered the possibility that the SNC meteorites are from Mars (e.g., Wasson and Wetherill 1979; McSween and Stolper 1980; Wood and Ashwal 1981). Three observations were considered highly indicative:

1. SNC meteorites belong to one group, as proven by many chemical and isotopic investigations, pointing to a common parent body.

2. All SNC meteorites are differentiated magmatic rocks, with some of them showing volcanic textures.
3. All SNC meteorites known at the time had young crystallization ages of 1.3 Gyr, thus requiring a parent body that still showed igneous activity at such a late time in solar system history.

Taken together, these arguments paint a picture in which the SNC meteorites are pieces of the planet Mars.

Additional evidence, which until 2004 was the most telling direct evidence, came from Viking 1, which landed on the surface of Mars about 30 years ago. Among other experiments, the concentrations and compositions of noble gases were measured by mass spectrometer (Nier et al. 1976; Owen et al. 1977). The agreement (within error) between the noble gas composition measured by Viking on Mars and the signatures found in constituents of some of the SNC meteorites (see below) constitutes rather conclusive evidence. Confirming the numbers obtained by Viking (and with better precision) has not been done until now since none of the instruments later sent to Mars were capable of analyzing the isotopic compositions of the atmospheric constituents.

In 2004, the rovers Spirit and Opportunity landed on Mars; at this time (early 2007) they are still exploring its surface. Results from these missions are continually adding further evidence that the SNC meteorites are Martian. In fact, rocks were found on Mars with chemical signatures identical to those of some of the Martian meteorites in our collections. For example, Opportunity investigated a rock named Bounce Rock and found geochemical characteristics, such as the Fe/Mg ratio, consistent with that of shergottites (Rieder et al. 2004). Nevertheless, to eliminate any remaining doubt, true Martian samples need to be investigated in comparison with the meteorites using high-accuracy analytical techniques. Although such definite proof will be possible only in the laboratory after a sample return mission, in this paper we will use the terms Martian meteorites and SNC meteorites interchangeably.

Shergottites are the most numerous among the Martian meteorites. Twenty-three of the currently known 33 Martian meteorites are classified as shergottites (Meyer 2003; Goodrich 2002; Russell et al. 2002, 2003, 2004). In the context of this paper, it is interesting that—as pointed out above—the similar "fingerprints" of noble-gas abundance patterns in shergottites and the data from the Viking mission have played a key role in establishing the SNC meteorites as Martian. Data from shock glasses in the shergottite Elephant Moraine (EET) A79001 led Bogard (1982) and Bogard and Johnson (1983) to conclude that Martian atmosphere is incorporated in this meteorite. Their findings were confirmed on the same meteorite by Becker and Pepin (1984a). Martian atmosphere was also later shown to be present in shock glasses of Zagami (Marti et al. 1995) and Shergotty (Bogard and Garrison 1998).

Atmospheric noble gases, both unfractionated and elementally fractionated, are not the only Martian noble gases trapped in the SNC meteorites. Another gas component is "Martian interior," first described by Ott and Begemann (1985) and Ott (1988), which is thought to be a component from the Martian mantle (Swindle 2002). A third signature, the origin and composition of which is not yet understood, was found in crushing experiments (Wiens 1988). Findings for nitrogen (e.g., Becker and Pepin 1984a, 1984b) are similar to those for the noble gases, showing the presence of a Martian atmospheric as well as an interior component (for a review on nitrogen, see Mohapatra [2004]). Table A1 in the Appendix provides an overview of previous publications on noble gases and nitrogen in the three shergottites studied here.

EXPERIMENTAL

Samples

Three Martian meteorites have been investigated: Shergotty, Zagami (normal lithology), and EETA79001 (lith. A). Shergotty and Zagami have been classified as basaltic shergottites by Goodrich (2002). Both contain mostly pyroxenes (>70%) and maskelynite (>20%), further mesostasis, and opaques (Meyer 2003). For EETA79001, the situation is more complex, as it contains three lithologies: while lithology C is shock melt glass and lithology B is regarded as basaltic shergottite, lithology A belongs to the olivine-phyric shergottites (Goodrich 2002). Our sample is of lithology A, which contains ~71% pyroxenes and ~17% maskelynite.

Three different samples of Shergotty and Zagami have been investigated: bulk, pyroxene, and maskelynite. For EETA79001, only bulk and pyroxene were investigated because the available sample volume was small, resulting in a separated amount of maskelynite less than 2 mg. These small amounts of sample will be measured after our new system has been installed, which is capable of dealing with very small amounts of krypton and xenon. Unfortunately, the bulk samples, due to the necessity of homogenization and splitting of the sample for parallel studies (Jochum et al. 2001; Bastian 2003; Fritz 2005), were ground to powder. Grinding can cause incorporation of noble gases from air, which has been observed by, e.g., Srinivasan et al. (1978) and Niemeyer and Leich (1976). Unfortunately, such gases can remain in the sample in degassing temperatures above 600 °C (Niedermann and Eugster 1992), and therefore disentanglement of the Martian air signature from the terrestrial air signature can be difficult.

The mineral separates did not suffer from this problem. They were obtained by handpicking from mildly crushed material. The purity of the separates was checked by scanning electron microscope (SEM) investigations. The separates were as pure as one can expect to obtain by handpicking of "big" grains. Crushing the grains down to a smaller grain size might have improved the purity, but would have increased the

danger of introducing air. We obtained 39 mg of maskelynite (grain size 0.05–1.2 mm) and 123 mg of pyroxene (grain size 0.1–1.5 mm) from Shergotty, 14 mg of maskelynite (grain size 0.5–1.5 mm) and 47 mg of pyroxene (grain size 0.2–1.0 mm) for Zagami, and (lith. A) 94 mg of pyroxene (grain size 0.1–0.7 mm) for EETA79001.

Measurement Procedures

For nitrogen and noble gas measurements, the mineral separates were wrapped in platinum foil. Platinum is used because it is inert not only against the noble gases but also against nitrogen. The foils have to be preheated to 700 °C in order to obtain low nitrogen extraction blanks. Blanks were somewhat variable, with typical values being $^{4}He = 2 \times 10^{-11}$ cc STP, $^{20}Ne = 2.5 \times 10^{-13}$ cc STP, $^{36}Ar = 4 \times 10^{-12}$ cc STP, $^{40}Ar = 1.2 \times 10^{-9}$ cc STP, $^{84}Kr = 6 \times 10^{-14}$ cc STP, $^{132}Xe = 2.5 \times 10^{-14}$ cc STP, $N_2 = 4 \times 10^{-11}$ pg. High- and low-temperature blanks were rather similar and within the range given here. Detailed blank corrections are based on blank values obtained from measurements of empty Pt foils heated in the temperature sequence 800 to 1800 °C.

The mineral separates were loaded to the sample holder and preheated at 130 °C for two days to remove adsorbed terrestrial contamination from the surface. Step-heating experiments were performed with details depending on the mineralogy and amount of sample (see Tables A2–A5). Samples were heated in at least three steps (holding the nominal temperature for 30 min at each step) in an iridium crucible. During heating, condensable gases were collected by a cold trap (–196 °C, filled with an SSM stainless steel mesh). After sample heating, the cold trap was separated from the line. The noncondensable gases, including the noble gases helium and neon, were exposed to three successive getters (one Ti, two SAES Zr-Al), then further cleaned by two cold traps (–196 °C, filled with charcoal) and finally measured in the mass spectrometer (MAP 215-50). For the Ne measurement, one of the cold traps remained connected to the spectrometer volume. During mass spectrometric analysis of Ne and He, gases adsorbed to the stainless steel mesh were released, with 5% admitted to the nitrogen line, where nitrogen was cleaned by oxygen released from heated copper oxide and finally admitted to the mass spectrometer for analysis after He and Ne. The remaining 95% admitted to the noble gas line were cleaned as the He and Ne fraction before and frozen to a charcoal filled cold trap close to the mass spectrometer. From this trap, argon, krypton, and xenon were released and measured successively. The analytical procedure will be described in more detail in a forthcoming paper by R. K. Mohapatra and co-workers.

The bulk samples were measured on a different system that does not allow measurement of nitrogen. Procedures were mostly equal except for wrapping the samples in Ni foil. Furthermore, the entire amount of gas was used for the noble gas measurements.

Data Reduction

The data reported below (see the Results section and Tables A2–A5) have been corrected for blanks and mass discrimination. In addition, interference correction was applied for HD and H_3 at ^{3}He, for $H_2{}^{18}O$ and doubly charged argon and CO_2 in Ne, for HCl and hydrocarbons at ^{36}Ar and ^{38}Ar, and also for hydrocarbons at ^{78}Kr. Errors include uncertainties due to variations in blank amounts and composition, uncertainties in the proper interference correction factors, and variations in mass discrimination and (for the amounts) sensitivity.

RESULTS

Results for the noble gases are summarized in Tables A2–A5. Nitrogen was only measured in Zagami mineral separates. We found 10.2 ± 0.6 ppm (pyroxene) and 24.7 ± 1.6 ppm (maskelynite) of N with $\delta^{15}N$ of 13.1 ± 0.7 and 22.7 ± 1.1, respectively. Nitrogen data will be discussed elsewhere.

Degassing Patterns

Stepwise-heating experiments can provide information about the nature and siting of the released gases. Helium almost quantitatively degasses in the low temperature steps (≤1000 °C) (Table A2). For neon, degassing patterns are not as clear-cut (Table A2). For the heavy noble gases, degassing patterns mostly distinguish between the adsorbed and the trapped component(s), which are released in different T-steps. In Fig. 1, the xenon release patterns are shown for the mineral separates. Xenon is used here because it is most critical regarding complete degassing. The ratio $^{129}Xe/^{132}Xe$ is used as an indicator to distinguish between the Martian atmospheric component and adsorbed air. However, this is only one dimension of a problem that has at least two dimensions, since it is difficult (considering the precision for small samples) to distinguish between trapped Martian interior gas and terrestrial atmosphere using this ratio alone. All diagrams indicate complete degassing, as the amount of gas released in the last step is small, if above blank level at all (Table A5). For the pyroxenes of all three meteorites $^{129}Xe/^{132}Xe$ is close to 1 in the T-steps ≤800 °C, which is indicative of adsorbed air. For the higher T-steps the ratio is slightly higher. The highest ratio of ~1.33 is observed in EETA79001 pyroxene. In contrast, both maskelynite separates show $^{129}Xe/^{132}Xe$ ratios of ~1.5 in their highest T-steps. A more detailed disentangling of the components will be done in the Discussion section.

Component Resolution

The noble gases were partitioned between trapped (plus radiogenic in the case of ^{4}He and ^{40}Ar) and cosmogenic

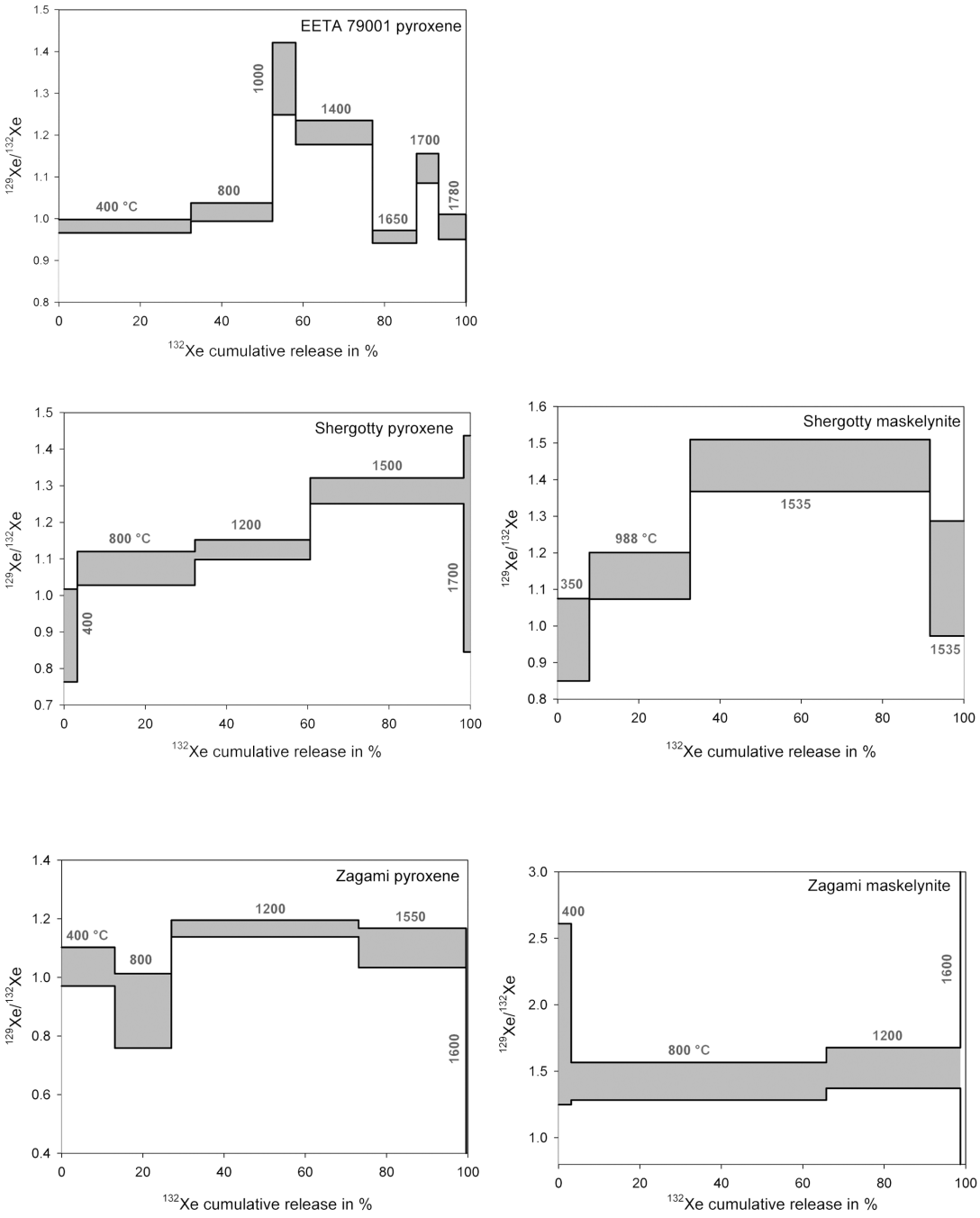

Fig. 1. Cumulative release plots from the mineral separates for ^{132}Xe as representative for the degassing patterns of heavy noble gases of the different phases. Plotted is the ^{129}Xe/^{132}Xe ratio versus cumulative fraction of ^{132}Xe released.

components. In the following discussion, "c" refers to cosmogenic and "tr" to trapped (+ radiogenic). For this ^{3}He was taken to be 100% cosmogenic, together with a ratio of $(^{4}He/^{3}He)_c = 5.2 \pm 0.3$ (Heymann 1967). Abundances of trapped ^{20}Ne and cosmogenic ^{21}Ne as well as estimates for the cosmogenic $(^{22}Ne/^{21}Ne)_c$ ratio were derived using $(^{20}Ne/^{22}Ne)_{tr} = 10 \pm 1$, $(^{21}Ne/^{22}Ne)_{tr} = 0.032 \pm 0.005$ (these values cover both air and reasonable values for Martian atmosphere), and $(^{20}Ne/^{22}Ne)_c = 0.80 \pm 0.05$ (GCR, chondritic range) (Wieler 2002). To check how much the derived $(^{21}Ne/^{22}Ne)_c$ depends on the assumed $(^{20}Ne/^{22}Ne)_c$, we checked (as an extreme value) use of $(^{20}Ne/^{22}Ne)_c = 1$ (SCR) (Garrison et al. 1995) and found this to result in decreasing the inferred $(^{21}Ne/^{22}Ne)_c$ by 2.1% (for bulk samples). However, lower $(^{21}Ne/^{22}Ne)_c$ can be due to causes other than low-energy irradiation; differences in chemistry

Table 1. Concentrations of cosmogenic isotopes (cc STP/g), production rates P (cc STP/g Myr), and cosmic-ray exposure ages T (Myr) determined in this study. Literature data for exposure ages are given for comparison. Literature data from: Eugster et al. (1997), data new in Eugster et al. (1997) (*), and data compiled by Eugster et al. (1997) (c). T in Myr. Elemental data for production rates from Meyer (2003), in detail for Shergotty from column Dreibus (1982), or Zagami from columns Smith (1984) and McCoy (1992), and for EETA79001 from column Warren (1997).

	Shergotty	Zagami	EETA79001, lith. A
$^{3}He_c$	$(3.81 \pm 0.16) \times 10^{-8}$	$(4.74 \pm 0.34) \times 10^{-8}$	$(9.72 \pm 1.22) \times 10^{-9}$
P_3	179.6×10^{-10}	178.6×10^{-10}	181.9×10^{-10}
T_3	2.12	2.65	0.53
$^{21}Ne_c$	$(5.44 \pm 0.30) \times 10^{-9}$	$(5.68 \pm 0.30) \times 10^{-9}$	$(1.40 \pm 0.01) \times 10^{-9}$
P_{21}	16.3×10^{-10}	18.6×10^{-10}	14.4×10^{-10}
T_{21}	3.34	3.05	0.97
$^{38}Ar_c$	$(2.99 \pm 0.16) \times 10^{-9}$	$(3.99 \pm 0.10) \times 10^{-9}$	$(0.59 \pm 0.04) \times 10^{-9}$
P_{38}	15.2×10^{-10}	16.0×10^{-10}	13.0×10^{-10}
T_{38}	1.97	2.50	0.46
$^{83}Kr_c$	$(1.45 \pm 0.18) \times 10^{-12}$	$(1.72 \pm 0.17) \times 10^{-12}$	$(0.30 \pm 0.14) \times 10^{-12}$
P_{83}	866.5×10^{-15}	793.8×10^{-15}	310.0×10^{-15}
T_{83}	1.67	2.17	0.98
$^{126}Xe_c$	$(22.2 \pm 1.4) \times 10^{-14}$	$(19.8 \pm 1.8) \times 10^{-14}$	$(0.5 \pm 1.4) \times 10^{-14}$
P_{126}	50.5×10^{-15}	53.9×10^{-15}	21.6×10^{-15}
T_{126}	4.40	3.67	
$T_{3–38}$	2.66	2.77	0.71
$T_{3–126}$	2.85	2.85	
$T_{3–38}$ lit.	2.71 ± 0.45^c $2.90 \pm 0.46^*$	2.72 ± 0.50^c	0.55 ± 0.16^c

and shielding may cause variations of the ratio similar to or even exceeding the variations due to different types of irradiation (see neon in the discussion). For argon, air or Martian atmosphere are possible choices as the trapped component; different choices for $(^{38}Ar/^{36}Ar)_{tr}$ within the range given in the literature (Bogard 1997; Wiens 1988) change the calculated $^{38}Ar_c$ and $^{36}Ar_{tr}$ abundances within error only (exceptions are the 800 °C-steps of Shergotty pyroxene, Shergotty maskelynite, and EETA79001 maskelynite). Here the value from Wiens et al. (1986) has been used: $(^{38}Ar/^{36}Ar)_{tr} = 0.2439 \pm 0.0112$, together with a cosmogenic ratio $(^{38}Ar/^{36}Ar)_c = 1.50 \pm 0.06$. Krypton was partitioned using $(^{83}Kr/^{84}Kr)_{tr} = 0.2025 \pm 0.0015$ (covering essentially all known trapped components) (cf. Ott 2002), and $(^{83}Kr/^{84}Kr)_c = 2.17 \pm 0.08$ (Ott 1988; Bogard et al. 1971). For xenon we assumed $(^{126}Xe/^{130}Xe)_{tr} = 0.0225 \pm 0.0025$ (covering the range for air, Martian atmosphere, solar, and AVCC) and $(^{126}Xe/^{130}Xe)_c = 1.02 \pm 0.06$ (Hohenberg et al. 1981; for a chondritic Ba/light REE ratio).

Cosmic-Ray Exposure Ages

We calculated cosmic-ray exposure ages using the isotopes ^{3}He, ^{21}Ne, ^{38}Ar, ^{83}Kr, and ^{126}Xe following the method of Eugster and Michel (1995) and Eugster et al. (1997). Our mean values for the ages obtained from ^{21}Ne and ^{38}Ar are 2.48 Myr for Shergotty, 2.73 Myr for Zagami, and 0.65 for EETA, lith. A. Mean values for ages from all five cosmogenic isotopes for Shergotty and Zagami are 2.70 and 2.81, respectively. These are in agreement with results found in the literature (e.g., Eugster et al. 1997). Detailed results are given in Table 1. Calculation of cosmic-ray exposure ages from mineral separates works quite well for the pyroxenes, giving essentially identical values. The empirical formulae cannot be applied to the feldspar separates, however, because in this case a significant amount of cosmogenic Ne is produced from Na, which is not included in the formulae.

DISCUSSION

Helium Loss

Helium contained in the solid or liquid precursors is lost during rock-formation processes, and one can safely assume the "memory" to have been reset. Implantation of He from the Martian atmosphere due to shock metamorphism cannot account for detectable amounts of He, because He constantly escapes the atmosphere of Mars. Its lifetime on Mars is 5×10^4 years only, and its concentration as low as 1.1 ± 0.4 ppm (Krasnopolsky et al. 1994). Therefore, ^{4}He in Martian meteorites has only two sources: radioactive decay of $^{238,235}U$ and ^{232}Th (accumulated since the rocks reached the closure temperature for He) and cosmic irradiation during passage from Mars to Earth. Knowing the crystallization age of a meteorite and assuming the system was closed since that time, the expected amount of radiogenic ^{4}He can be calculated from the amounts of $^{238,235}U$ and ^{232}Th. In a parallel study (Jochum et al. 2001) U and Th were measured by spark source-mass spectrometry and can be used for these calculations. The contribution to ^{4}He from cosmic irradiation can be estimated

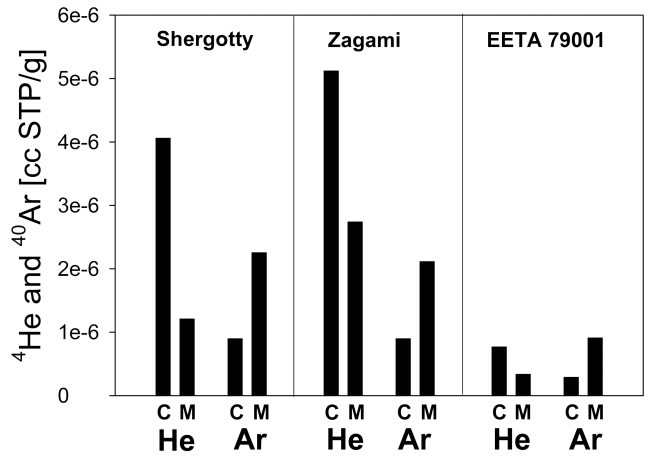

Fig. 2. Helium loss and argon loss/gain. C refers to the calculated concentration as expected from radioactive decay of U, Th, and K, respectively, M to the measured concentration. Only data for the bulk samples are shown; for mineral separates see text.

from the amount of ^{3}He: ^{3}He is almost completely cosmogenic, while ^{4}He is produced by cosmic irradiation with a ratio of $(^4He/^3He)_{cosm}$ = 5.2 (Heymann 1967) or 6.1 ± 0.3 (Alexeev 1998, 2005). For the Martian meteorites we have been using the lower value 5.2. This seems more realistic, at least for Martian meteorites, because using the higher value leads to negative inferred amounts of radiogenic ^{4}He for at least two cases in our complete data set of 13 different Martian meteorites from all classes (Schwenzer 2004): Allan Hills (ALH) A77005 and Dar al Gani (DaG) 476, with measured ^{4}He/^{3}He ratios of 4.18 ± 0.12 and 4.88 ± 0.20, respectively. Note that Eugster et al. (2002) found a similarly low ratio for ALHA77005, and the low ratio ~5.0 measured by Eugster et al. (1997) for yet another Martian meteorite, Queen Alexandra Range (QUE) 94201. Furthermore, the measured amount of ^{3}He in Shergotty and Zagami maskelynite indicates severe loss of cosmogenic helium from this phase.

A comparison of the resulting "observed" radiogenic ^{4}He with the expected amount of radiogenic ^{4}He in the meteorite indicates significant helium loss (Fig. 2). Losses amount to ~70% for Shergotty, ~47% for Zagami, and ~56% for EETA79001. As helium is easily lost due to high diffusion rates even at relatively low temperatures in silicates and glass melts (Ozima and Podosek 2002), a possible scenario is that the helium loss is a result of the shock metamorphism to which the meteorite was exposed during the launching event (Schwenzer et al. 2004). The diffusion coefficient for helium is higher than for argon, so helium is lost more easily than Ar and other heavy noble gases (Alexeev 2005). The field of investigating shock pressures and post-shock temperatures has had some lively debates and is controversial (e.g., Malavergne et al. 2001; Fritz et al. 2003; El Goresy et al. 2004; Beck et al. 2005, Fritz et al. 2005). It is worth noting, therefore, that our interpretation is independent of the method with which the shock pressure is estimated and also independent of the absolute numbers of peak shock pressure and temperature.

As there is "no" He in the Martian atmosphere (Krasnopolsky et al. 1994), shock causes a "one-way" effect for helium. This is different for argon, which is present in the Martian atmosphere in significant abundance. From ^{40}K decay—K abundance data again from Jochum et al. (2001)—similar calculations can be made, but a surplus of ^{40}Ar is observed instead of loss. We observe ^{40}Ar "gain" of 151% for Shergotty, 136% for Zagami, and 215% for EETA79001. This suggests the implantation of atmospheric ^{40}Ar in the course of the impact event and corresponds to the observation of Martian atmospheric signatures in these meteorites (e.g., Bogard and Johnson 1983; Becker and Pepin 1984a; see also discussion of argon data).

Neon: The Influence of Solar Cosmic Rays

Trapped components contributing to Ne are Martian atmosphere and Martian interior and (possibly) terrestrial air. Furthermore, the not-yet-understood component found by Wiens (1988) when crushing EETA79001 glass can contribute to the budget. The rather high abundance of sodium in feldspar may have a special effect on the isotopic composition of spallogenic Ne released at low extraction temperatures (Smith and Huneke 1975).

Figure 3a shows our data for Shergotty, Zagami, and EETA79001 in a diagram of ^{20}Ne/^{22}Ne versus ^{21}Ne/^{22}Ne. There is clear evidence for the presence of a trapped component in several degassing steps. However, since the isotopic difference between Ne in the Martian atmosphere and in terrestrial air is small (see Fig. 3a and references in the caption), it is impossible to distinguish which of the two is present based on Ne isotopes alone. In order to get some idea, we have also taken into account the signatures observed in the other noble gases. For the 400 °C step of Zagami pyroxene and for the low-temperature step of Shergotty maskelynite, heavy noble gas data (see following sections) show the dominant presence of air, so we suspect the same may be the case for Ne. Only for the 1600 °C step of Zagami maskelynite (arrow in Figs. 3a and 3b) does there appear to be a noticeable contribution from Martian atmospheric Ne.

The spallation composition shown in Fig. 3a covers the range from 0.80 to 0.95 in ^{21}Ne/^{22}Ne, which is the range for Ne produced by galactic cosmic rays (GCR) as usually observed in bulk samples of chondrites (e.g., Wieler 2002). Among our data points, only about half fall into this range, while the others show lower ratios of cosmogenic ^{21}Ne/^{22}Ne. In principle, there are two possible reasons.

First, there could be differences in chemical composition. Magnesium, which is a dominant target element in chondrites, is comparably low in many SNCs; as a result the

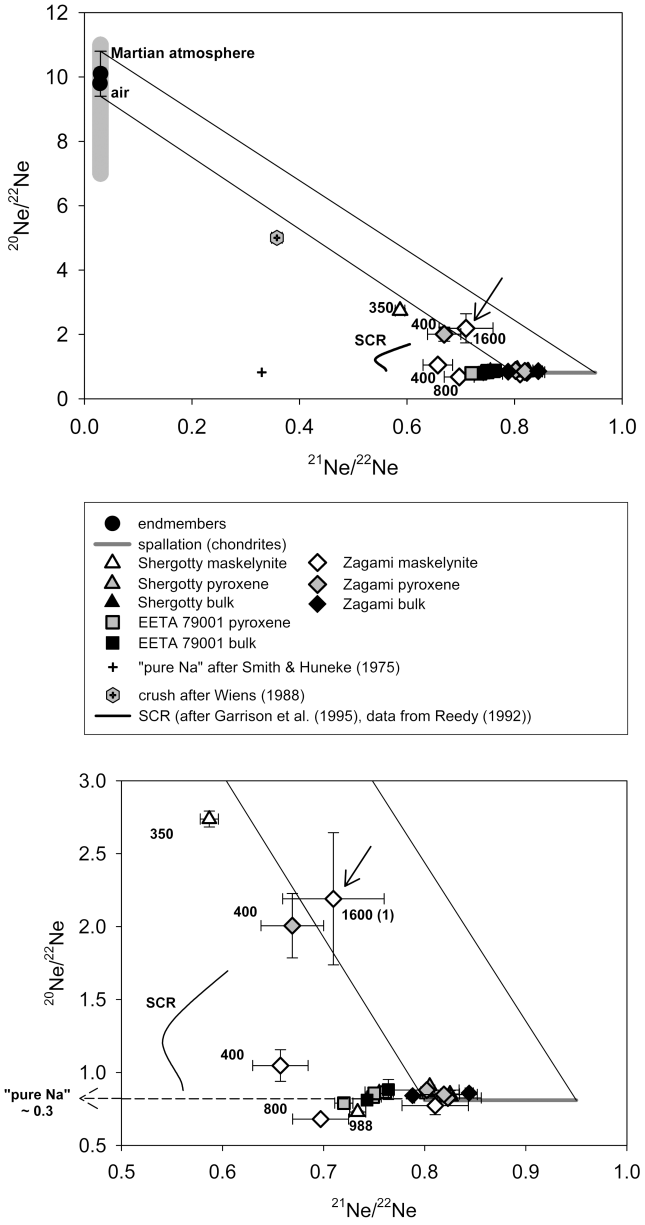

Fig. 3. a) Neon isotopic data for Shergotty (maskelynite, pyroxene, and bulk), Zagami (maskelynite, pyroxene, and bulk) and EETA79001 lith. A (pyroxene and bulk). Extraction temperatures in °C are indicated for a few specific cases. Shown in the upper left part are the trapped components air (lower black dot) and Martian atmosphere (upper black dot; Bogard and Garrison, 1998; Swindle, 2002). The gray line indicates the range of results for Martian atmospheric Ne given in the literature, which ranges from $^{20}Ne/^{22}Ne$ = 7 to 11 (Swindle et al. 1986; Wiens et al. 1986; Pepin 1991; Ott and Löhr 1992; Bogard and Garrison 1998; Mohapatra et al. 2003; Schwenzer et al. 2005; Park and Nagao 2006). Also shown is the SCR-Ne signature (after Garrison et al. 1995; data from Reedy 1992) as well as the $^{21}Ne/^{22}Ne$ ratio derived by Smith and Huneke (1975) for pure sodium spallation. b) Lower right part near spallation composition, enlarged. The arrow in Figs. 3a and 3b points to the 1600 °C data point for Zagami maskelynite, which may show evidence for trapped Martian Ne.

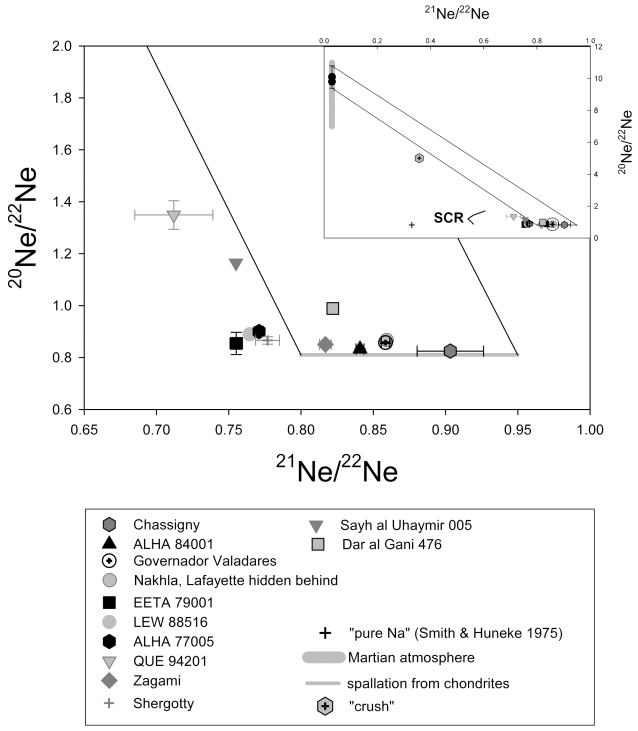

Fig. 4. Neon isotopic data for thirteen Martian meteorites (Schwenzer 2004; LEW 88516 from Ott and Löhr 1992). For endmembers and references, see Fig. 3. Six meteorites (QUE 94201, EETA79001, LEW 88516, ALHA77005, and Shergotty) out of thirteen show $(^{21}Ne/^{22}Ne)_c$ ratios lower than the GCR spallation range observed in chondrites.

statement by Garrison et al. (1995) that Al and Na (both giving low $^{21}Ne/^{22}Ne$) are "relatively less important" does not always apply in the case of the SNCs. In addition, we call attention to the fact that, apart from its influence on the isotopic composition, Na is not taken into account in empirical formulae for Ne production rates (e.g., Eugster 1988; Eugster and Michel 1995; Schultz et al. 2005).

Second, there could be contributions from solar cosmic ray (SCR) spallation, which is only rarely observed in chondrites (e.g., Wieler 2002), but has been inferred for some shergottites (Garrison et al. 1995; Eugster et al. 1997). Unfortunately the most up-to-date work on SCR production rates considers the target elements Mg, Al, and Si only (Reedy 1992).

The region near the spallogenic corner is shown enlarged in Fig. 3b. For the mineral separates differences due to chemistry are obvious. Maskelynite, especially in low temperature steps, tends to show lower cosmogenic $^{21}Ne/^{22}Ne$ ratios than pyroxene and bulk of the same meteorite. Nevertheless, the data in this representation do not allow us to clearly distinguish the chemical composition effect from the influence of SCR.

We next turn to the situation for bulk SNC meteorites in general, before getting back to the mineral separates. Figure 4 shows our complete data set including data for other SNC

Table 2. Minimum radii and cosmogenic $(^{21}Ne/^{22}Ne)_c$ in suite of 13 Martian meteorites.

Name	Class[a]	Recovered mass[b] (kg)	Density[c] (g/cm^3)	Min. radius[d] (cm)	Min. category[e] (cm)	$(^{21}Ne/^{22}Ne)_c$[f]	Min. pre-atmosph. radius[g] (cm)
Chassigny	Chassignite	4	4.7	5.9	5	0.906 ± 0.024	24 ± 2
ALHA 84001	Orthopyroxenite	1.93	3.3	5.2	5	0.834 ± 0.005	
Lafayette	Nakhlite	0.8	3.3	3.9	5	0.826 ± 0.007	
Nakhla	Nakhlite	10	3.3	9.0	10	0.865 ± 0.006	22 ±1
Governador Valadares	Nakhlite	0.158	3.3	2.3	5	0.864 ± 0.006	
Dar al Gani 476	Olivine phyric shergottite	>6–7 pieces	3	7.8	10	0.839 ± 0.015	
Sayh al Uhaymir 005	Olivine phyric shergottite	>10, about 7 pieces	3	9.3	10	0.806 ± 0.005	25 ± 2
EETA79001, Lith. A	Olivine phyric Shergottite	7.94	3	8.6	10	0.760 ± 0.007	
LEW 88516	Lherzolitic shergottite	0.0132	3	1.0	5	0.772[h] ± 0.005	
ALH 77005	Lherzolitic shergottite	0.482	3	3.4	5	0.779 ± 0.006	
QUE 94201	Basaltic shergottite	0.012	3	1.0	5	0.755 ± 0.030	24 ± 1
Zagami	Basaltic shergottite	~18	3	~11.3	15	0.821 ± 0.006	23 ± 1
Shergotty	Basaltic shergottite	5	3	7.4	10	0.785 ± 0.010	23 ± 1

[a]Goodrich (2002).
[b]Meyer (2003).
[c]Estimated from mineralogical composition.
[d]Radius of a sphere with the mass in column 3 and density in column 4.
[e]The data in Leya et al. (2000) for radii: 5, 10, 15, 25, 32, 40, 50, 65, and 85 cm. For "minimum category" we have used the radius, closest to the minimum radius in column 5. This refers to the range shown as solid line in Fig. 4.
[f]Data for bulk samples from Schwenzer (2004).
[g]Pre-atmospheric size from Eugster et al. (2002).
[h]Data from Ott et al. (1996).

meteorites, which will be discussed in more detail in a forthcoming separate publication. Obviously, for six out of the thirteen Martian meteorites, cosmogenic $(^{21}Ne/^{22}Ne)_c$ is lower than the spallation field from chondrites indicates. For further evaluation, whether this is caused by chemistry or SCR, it is necessary to check the influence of chemistry in more detail. We have done so using the modern production rates for GCR-produced Ne as a function of shielding and chemical composition given by Leya et al. (2000) that were not yet available to Garrison et al. (1995). In contrast to earlier similar "physical models," the model of Leya et al. (2000) fairly reliably predicts not only production *rates* but also Ne isotopic *ratios*. For example, production at depth ~10 cm in a 25 cm L chondrite (as other similar cases), reproduces the "normal shielding" value $(^{22}Ne/^{21}Ne)_c = 1.11$, which is also in agreement with the empirical model of Graf et al. (1990).

GCR spallation on Na produces $(^{21}Ne/^{22}Ne)_c$ significantly lower than that produced on the main target elements Mg and Si. The abundance of Na relative to the latter is often relatively high in SNC meteorites when compared to chondrites, hence the influence of Na content on the Ne isotopic composition is correspondingly larger. For example, neglecting the target element Na in the Leya calculations predicts a $(^{21}Ne/^{22}Ne)_c$ ratio for a 5 cm radius L chondrite that is too high by between 0.5% (surface) and 1.2% (center), while for an equivalent target having the composition of Shergotty the effect ranges between 0.9% (surface) and 1.8% (center). For a meteoroid having a radius of 40 cm (note the minimum 23 cm radius of Shergotty, Eugster et al. 2002), on the other hand, the corresponding numbers are larger: 2.3 to 3.4% (surface to center with L chondrite composition) versus a quite significant 4.4 to 6.1% (Shergotty chemical composition).

In a simplified picture, the trend of $(^{21}Ne/^{22}Ne)_c$ as a function of size and depth is largely controlled by the mineralogical makeup of a given sample. This is because in the elemental production rates of Leya et al. (2000) two different types of patterns show up: for production on Na, $(^{21}Ne/^{22}Ne)_c$ decreases with increasing radius and shielding depth; the same behavior is shown by Al (also with relatively low $(^{21}Ne/^{22}Ne)_c$). Since abundances of Na and Al run largely parallel with feldspar content of a given sample, the effects of both elements add up. Production on magnesium and silicon, on the other hand, shows the opposite trend. Iron (decreasing with radius and depth) and calcium (increasing) have only minor influence, because production is much lower than on Na, Mg, Al, and Si.

More to the point, we have calculated $(^{21}Ne/^{22}Ne)_c$ for the individual chemistry of each of the 13 meteorites from our complete study, based on the Leya et al. (2000) GCR model (Table 2). For the chemical composition mostly the mean values in the compilation of Lodders (1998) are used. Exceptions are as follows: a) Lafayette: the only value for Na has been obtained by Boctor et al. (1976) on fusion crust. As crust may be depleted in Na, for the bulk rock a value of 0.42% (by weight) has been adopted, based on petrologic investigation and Na_2O content of plagioclase (Treiman 2005; A. H. Treiman, personal communication). b) Sayh al Uhaymir (SaU) 005 and Dar al Gani 476: data from Dreibus et al. (2000) and from Zipfel et al. (2000) are used.

The predicted GCR-produced Ne in all but one case (QUE 94201) shows increasing $(^{21}Ne/^{22}Ne)_c$ ratios with increasing radius and depth, which can be explained by the dominance of mafic Mg-, Si-rich minerals (pyroxene, olivine). In Fig. 5 we have plotted $(^{21}Ne/^{22}Ne)_c$ values (calculated as described in the chapter "component resolution") from our own complete data set (diamonds) (Table 2) as well as from data for the same meteorites taken from the literature (compilation of Schultz and Franke 2004; + signs). These are compared to the range of possible values produced by GCR. The range is bounded on the high mass end by a radius $r = 85$ cm, the maximum in Leya et al. (2000). On the low mass side, we chose 10 cm for Nakhla, DaG 476, SaU 005, EETA79001, and Shergotty; we chose 15 cm for Zagami. These are based on "minimum radii" calculated from the recovered masses and assuming spherical geometry of 9, 8, 9, 9, 7, and ~11 cm (Table 2). For the other meteoroids, the calculations include radii down to 5 cm, the minimum in the Leya et al. (2000) compilation. Also shown is the resulting restricted range if one follows Eugster et al. (2002) who, based on the production of neutron capture ^{80}Kr, derived minimum radii between 22 and 25 cm for Chassigny, Nakhla, SaU 005, QUE 94201, Zagami, and Shergotty.

For Chassigny, ALH 84001, and the nakhlites there is a "direct match" in that the observed $(^{21}Ne/^{22}Ne)_c$ lies in the "allowed range" for production by GCR. For these five (out of thirteen meteorites), experimental values are reasonably compatible with values expected from GCR irradiation, and there is no need to invoke a contribution from solar cosmic rays. The situation is different for the eight shergottites, where most experimental $(^{21}Ne/^{22}Ne)_c$ ratios are lower than the calculated GCR range. These are discussed in detail below.

Olivine-Phyric Shergottites DaG 476, EETA79001, and SaU 005

Most data plot lower than the GCR range, but the latter two show a wide range with some values even above the allowed range. Data points at the high end can only be explained as the result of mineralogical variability and fortuitous measurements of pieces with unusual composition.

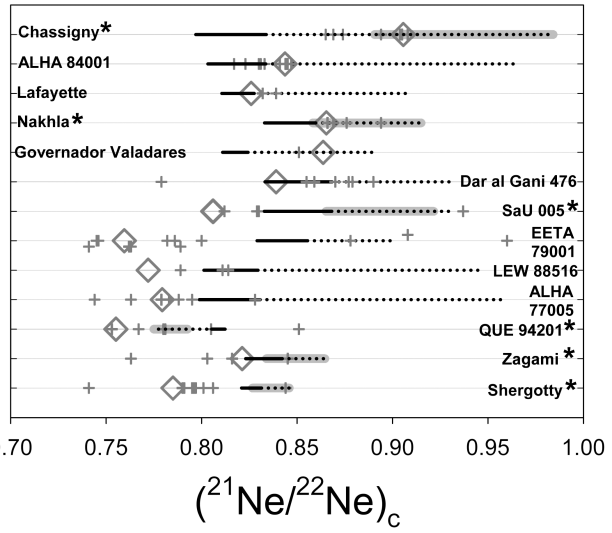

Fig. 5. Cosmogenic $(^{21}Ne/^{22}Ne)_c$ for the thirteen Martian meteorites shown in Fig. 4 as derived from measured Ne, compared with the range of possible ratios according to production rates of Leya et al. (2000) for GCR spallation (cf. Table 7). Open diamonds are $(^{21}Ne/^{22}Ne)_c$ ratios from Schwenzer (2004), while gray crosses are $(^{21}Ne/^{22}Ne)_c$ ratios calculated from data of various authors as given in the compilation of Schultz and Franke (2004). For EETA79001, lith. A data are plotted on the line, lith. C data slightly below, lith. B data slightly above. Thick solid lines indicate the theoretical $^{21}Ne/^{22}Ne$ range for the size, which fits most closely to the calculated minimum radius derived from the recovered mass. Dotted lines show range of ratios for radii up to 85 cm (see text and Table 7). Meteorites with an asterisk have a pre-atmospheric radius of at least 22–25 cm according to ^{80}Kr measurements by Eugster et al. (2002). For these cases the light gray field in the background shows the range predicted for a radius of 25 cm to the maximum range by Leya et al. (2000).

For SaU 005, low values may also be explained if GCR production occurred in a meteoroid with an *effective* radius of ~5 cm, smaller than the "minimum radius" calculated from the recovered mass assuming spherical shape. This is because production in a meteoroid of nonspherical shape such as an ellipsoid can be approximated by production in a sphere with smaller radius (Kim et al. 2005). However, for DaG 476 and EETA79001 even this is not sufficient to explain the observed low $(^{21}Ne/^{22}Ne)_c$ ratios.

Lherzolithic Shergottites (LEW 88516 and ALHA 77005) and Basaltic Shergottites (QUE 94201, Shergotty, Zagami)

For all of these, most measured $(^{21}Ne/^{22}Ne)_c$ values are lower than the GCR minimum predicted values. Varying the chemistry within the compositional range given in Meyer (2003) does not change this situation. Also, invoking nonspherical shape again and considering effective radii down to 5 cm as for SaU 005, while extending the range to lower values, still leaves most measured values outside the GCR range. Evidently neon systematics suggests that contributions from SCR are required, although for QUE

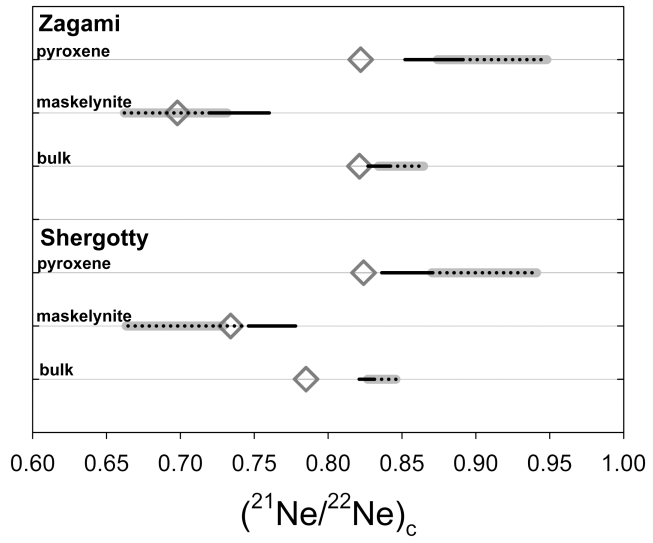

Fig. 6. Measured $(^{21}Ne/^{22}Ne)_c$ and calculated $(^{21}Ne/^{22}Ne)_{GCR}$ ratios for mineral separates and bulk samples of Shergotty and Zagami. Otherwise like Fig. 5. The chemical compositions of the bulk meteorites have been taken from the compilation of Lodders (1998). The mineral chemistry for Shergotty maskelynite and pyroxene is from Stöffler et al. (1986), and that for Zagami is from Stolper and McSween (1979).

94201 this is not supported by cosmogenic radionuclide data (see Kring et al. 2003 and discussion therein).

Mineral Separates (Shergotty and Zagami)

Coming back to the mineral separates, the results for cosmogenic $(^{21}Ne/^{22}Ne)_c$ in the Shergotty and Zagami separates (Fig. 6) support the conclusions based on bulk-meteorite data. For a comparison with the GCR model predictions, the mineral chemistry for Shergotty maskelynite and pyroxene was taken from Stöffler et al. (1986), and that for the Zagami minerals from Stolper and McSween (1979). Results for pyroxene again strongly suggest the influence of solar cosmic rays. No clear evidence is visible in the case of maskelynite, but this simply may be due to the fact that for maskelynite (high in Na) the ratio from GCR irradiation is low already, so it is less sensitive to the addition of another component (SCR) with low $(^{21}Ne/^{22}Ne)_c$.

Presence of spallogenic Ne produced by SCR irradiation requires that the meteoroids suffered only little ablation. Its detection also implies that the samples that have been analyzed must have been close (maximum 2–3 cm) (cf. Hohenberg et al. 1978; Reedy 1992) to the pre-atmospheric surface. This may not be too surprising for the small ones (LEW 88516, ALHA77005, QUE 94201), since the outermost 3 cm of the meteorite make up the meteorite's main mass, and, assuming negligible ablation, also the main portion of the meteoroid. For the larger ones the chance to sample the outermost 3 cm (of the meteorite) can be estimated as roughly 20–40%, if random sampling is assumed. While this agrees well with the distribution of data points for DaG 476 and SaU 005, for EETA79001, Shergotty, and Zagami more than 70% of the data points are lower than the calculated range.

Garrison et al. (1995) have discussed several possibilities for the apparent prevalence of SCR contributions in shergottites. Short cosmic-ray exposure times may have helped. This is because space erosion constantly removes material from the surface and the SCR component within them. Hence material currently in the outermost few centimeters received its SCR component later (and only for a fraction of the total cosmic-ray exposure), but contains GCR-produced nuclides that accumulated during the full cosmic-ray exposure time. Another possibility is that SCR fluxes were higher in the past few million years. The difference in exposure ages (e.g., Eugster et al. 1997; Nyquist et al. 2001) between the shergottites and the chassignite/nakhlite group of meteorites allows for both of these scenarios. However, there are non-Martian meteorites, which are also small and also have short exposure ages that do not show evidence for a SCR contribution, calling these explanations into question (Garrison et al. 1995; Rao et al. 1994). What may be required is unusual orbital parameters that may have resulted in slow entry velocities and very little ablation. Orbits of Martian meteorites differ from those of meteorites from other sources, as Mars is a relatively small planet with a comparatively excentric orbit. According to the models of Gladman (Gladman et al. 1996; Gladman 1997), a meteoroid remains in the gravitational field of Mars for only about 10^5 years and reaches Earth in a time span between 16,000 and 30 million years (after which collision with Earth gets highly improbable). Those special orbits could also have led the meteoroids closer to the Sun, resulting in higher SCR fluxes (Garrison et al. 1995). In fact, the low abundances of cosmogenic ^{3}He in the maskelynites (only 20–25% of those in the bulk) (Table A2) may be indicative of such orbits leading to loss of ^{3}He due to solar heating. It may also be of interest to explore the influence of the specific types of ejection mechanisms required to lift off meteorites from a planetary rather than an asteroidal body (Artemieva and Ivanov 2004; Wetherill and Chapman 1988) and whether these ejection mechanisms may have led to nonspherical shapes with a higher fraction of near-surface material recording the effects of SCR.

Argon

The bulk of argon (both ^{36}Ar and ^{38}Ar) from Zagami maskelynite is released in the 1200 °C step (Table A3). For Shergotty maskelynite, where the 1200 °C step was omitted because the amount of sample was small, main release was at the next higher temperature, 1535 °C. The composition of maskelynite in Shergotty and Zagami is about $An_{50}Ab_{50}$ (Meyer 2003). The melting point for such plagioclase is clearly above 1100 °C (Deer et al. 1992), so the observed

degassing temperatures clearly reflect the melting of plagioclase. The melting temperature of pyroxene is higher, and the fact that main gas release from pyroxene is in T steps above 1400 °C clearly reflects this. Unfortunately, due to restrictions concerning the oven system at the time of measurement, the pyroxene separates of Shergotty and Zagami were only heated up to 1600 °C. In the case of EETA79001, there is nominal release of some trapped gas at 1700 °C and at 1780 °C, after a 1650 °C step, which is at nominal blank level (Table A3). As the compositional range of pyroxenes in these meteorites is largely the same (cf. compositional diagrams V-4 [Shergotty], VI-5 [Zagami], and IX-13 [EETA79001] of Meyer 2003), we cannot exclude with certainty that, if present, we missed such a type of trapped gas in the case of Shergotty and Zagami pyroxenes. It appears unlikely, however, since pyroxenes of the given compositions melt between 1250 and 1400 °C (Deer et al. 1992). Instead, since olivine is much more abundant in EETA79001 (lith. A) than in Shergotty and Zagami, the gas observed in EETA79001 at 1700 °C is more likely to derive from olivine than from pyroxene. Even more likely, however, is that the high-T trapped gas in EETA79001 pyroxenes is an artifact caused by underestimation of the blank. These high extraction temperatures were only rarely used and are only slightly lower than the degassing temperature of our Ir system for N and noble-gas extraction. This interpretation is supported by the isotopic composition of the Ar, which in these steps is indistinguishable from that of air. Consequently, the 1700 °C, 1780 °C, and (blank-level) 1650 °C steps of EETA79001 pyroxene have not been included in the calculation of the totals for Ar (Table A3).

In all the mineral separates, ^{36}Ar and ^{38}Ar are dominated by the cosmogenic component. Although the chemical compositions of pyroxene and maskelynite are completely different, $^{38}Ar_c$ is present in comparable concentrations in pyroxene and maskelynite. This is as expected from production rates for $^{38}Ar_c$ (Freundel et al. 1986; Eugster and Michel 1995), and the relative abundance of K, Fe, and Ca (the latter approximately the same in both minerals) (Terribilini et al. 1998). Trapped $^{36}Ar_{tr}$ is also rather similar in pyroxene and maskelynite (Table 3). ^{40}Ar, however, is higher by a factor of 2.3 (Shergotty) and 2.9 (Zagami) in maskelynite than in pyroxene. This is also the only isotope that does not show a maximum of degassing at or above the melting temperature of the respective mineral. Instead the amount of ^{40}Ar is almost the same in all T-steps. $^{40}Ar/^{36}Ar_{tr}$ is low, in the low-temperature steps, most probably reflecting air contamination, and shows a uniform (and high) ratio in the higher T-steps (Tables A3 and 3). Thus, while the (mostly cosmogenic) ^{36}Ar and ^{38}Ar generally occupy positions within the structures of the mineral phases, ^{40}Ar may be, at least in part, located close to the surface. The diverging degassing patterns reflect the different sources of the isotopes: whereas the trapped component is incorporated during mineral growth, cosmogenic $^{38}Ar_c$ is produced from nuclides in the structure of the phase. Furthermore, Ar from the atmosphere is incorporated during shock metamorphism. In fact, in agreement with our conclusion above, Gilmour et al. (2001) infer from their study of Nakhla and comparison with Chassigny and ALH 84001 that the Martian atmospheric component introduced by shock is located close to grain surfaces.

In principle, it is also possible to obtain Ar-isochron ages, which date the rock formation, from Martian meteorites by plotting the ratio of trapped plus radiogenic ^{40}Ar to trapped ^{36}Ar ($^{40}Ar_{tr\,+\,rad}/^{36}Ar_{tr}$) versus $K/^{36}Ar_{tr}$, the ratio of potassium to trapped ^{36}Ar (Terribilini et al. 1998). However, it is unlikely that these agree with ages from undisturbed (by shock) isotopic systems. Our isochron "ages," based on the data points for maskelynite and pyroxene each, are ~130 Myr for Shergotty and ~150 Myr for Zagami. An age could not be calculated for EETA79001 (lith. A) because we do not have data for maskelynite. These ages are lower than the widely accepted crystallization ages of about 165 Myr for Shergotty and 207 Myr for Zagami (Nyquist et al. 2001; cf. Meyer 2003), and thus below the range of published ages obtained by different techniques and from different minerals, which show a range between 600 and 147 Myr for Shergotty and 180 and 230 Myr for Zagami (Meyer 2003). A possible shortcoming in our approach is that the data for K had to be taken from the literature (Table 4) and were not obtained on the same sample as the noble gases. In addition, shock may have influenced Ar content and distribution. Nevertheless, within the respective uncertainties our result for Shergotty is compatible with the isochron "age" of Terribilini et al. (1998) of 196 ± 40 Myr.

The effect of Ar implantation from the Martian atmosphere is clearly seen in the three-isotope-diagram $^{129}Xe/^{132}Xe$ versus $^{36}Ar_{tr}/^{132}Xe$ of Fig. 7. Clearly, there is more shock-implanted Ar in maskelynite than in pyroxene, most likely because this phase underwent more intense structural changes during the shock event. In addition, Fig. 7 shows the effect of the unwanted introduction of noble gases into the bulk samples during the grinding procedure. As grinding introduces more Xe than Kr and more Kr than Ar (relative to the starting composition), bulk samples are shifted to the left in comparison to pyroxene. While for argon the effect of grinding the bulk sample is still comparably small, the Kr and Xe results for bulk are compromised by the sample preparation more seriously (see below).

Krypton and Xenon

Unfortunately, the effect of introducing fractionated air by grinding the sample can be seen in our whole-rock data like in a textbook example (Fig. 7; Tables A4 and A5). This shows up, e.g., in that the amounts of ^{84}Kr as well as ^{132}Xe in the whole-rock samples are much higher than expected from

Table 3. Trapped and cosmogenic Ar components. Calculated using $(^{38}Ar/^{36}Ar)_{tr} = 0.2439 \pm 0.0119$ for the Martian trapped component (Wiens et al. 1986) and $(^{38}Ar/^{36}Ar)_c = 1.50 \pm 0.06$ (see text). Concentrations are given in 10^{-9} cc STP/g.

Sample	Temperature (°C)	$^{36}Ar_{tr}$	$^{38}Ar_c$	$(^{40}Ar/^{36}Ar)_{tr}$
Shergotty pyroxene (123.12 mg)	800	0.353 ± 0.029	0.049 ± 0.006	2021 ± 158
	1200	0.212 ± 0.024	0.287 ± 0.014	1810 ± 200
	1500	0.243 ± 0.104	2.577 ± 0.112	2054 ± 883
	1700	0.040 ± 0.007	0.074 ± 0.008	651 ± 107
	Sum	0.848 ± 0.111	2.986 ± 0.114	1914 ± 250
Shergotty maskelynite (39 mg)	988	0.589 ± 0.065	0.699 ± 0.036	3160 ± 335
	1535	0.500 ± 0.101	2.116 ± 0.092	3738 ± 756
	Sum	1.169 ± 0.052	2.811 ± 0.101	3215 ± 194
Zagami pyroxene (46.9 mg)	800	0.146 ± 0.020	0.068 ± 0.009	4013 ± 521
	1200	0.122 ± 0.043	0.790 ± 0.064	2322 ± 816
	1550	0.072 ± 0.075	1.920 ± 0.083	1509 ± 1588
	Sum	0.339 ± 0.089	2.779 ± 0.105	2875 ± 507
Zagami maskelynite (14 mg)	800	0.080 ± 0.024	0.156 ± 0.037	6106 ± 1593
	1200	0.239 ± 0.107	1.662 ± 0.162	6490 ± 2893
	1600	0.162 ± 0.076	0.921 ± 0.136	5076 ± 2334
	Sum	0.481 ± 0.134	2.739 ± 0.214	5950 ± 1630
EETA79001 pyroxene (94.3 mg)	800	0.131 ± 0.015	0.057 ± 0.006	1847 ± 217
	1000	–	0.087 ± 0.019	–
	1400	–	0.389 ± 0.060	–
	Sum	0.131 ± 0.011	0.533 ± 0.063	4012 ± 476[a]

[a]Includes ^{40}Ar released at 1000 °C and 1400 °C (cf. Table 3).

the weighted averages of pyroxene and maskelynite. The isotopic signature especially of xenon, showing lower $^{129}Xe/^{132}Xe$ in the whole rock than in all separates, proves the additional component to be air. Therefore the whole-rock data are not further discussed.

Looking at the degassing patterns of Kr and Xe from the mineral separates, the contribution from terrestrial atmosphere can be discerned in the first temperature step (e.g., by the low $^{129}Xe/^{132}Xe$) (Tables A3 and A4). The main amount of Martian Kr and Xe is released in T-steps ≥1200 °C and therefore is related to the melting temperature of the phases. Amounts of ^{84}Kr and ^{132}Xe are higher in Shergotty maskelynite than in Shergotty pyroxene. Differences in Kr isotopic composition are due to the higher abundance of cosmogenic Kr in maskelynite, due to the distribution of the trace target elements Sr, Y, and Zr. The situation is similar in Xe, where spallogenic contributions in the light isotopes are more clearly visible in maskelynite than in pyroxene.

As for Ar, the implanted Martian atmosphere can be detected by its isotopic signature, i.e., by the high $^{129}Xe/^{132}Xe$ ratios (Fig. 8). As ^{129}Xe (in contrast to ^{40}Ar) is only from two sources (Martian interior and atmosphere), it is straightforward to determine the amount of implanted ^{129}Xe. For EETA79001 pyroxene as well as Shergotty pyroxene and maskelynite, the degassing patterns (Fig. 1) show elevated $^{129}Xe/^{132}Xe$ in the high-T steps. For Zagami the picture is not that clear; only maskelynite shows a high a $^{129}Xe/^{132}Xe$ ratio >1.4, but $^{129}Xe/^{132}Xe$ in pyroxene does not exceed 1.2. The amounts of $^{129}Xe^*$ calculated as excess over $^{129}Xe/^{132}Xe = 1.03$ (Martian interior; Ott 1988) are shown in Table 4. In summary, for the heavy noble gases the study on mineral separates shows the maskelynite to contain abundant Martian atmospheric gas, but some implanted atmosphere can also be found in pyroxene.

Martian Interior Argon

Interestingly, our mineral separate data, particularly for Shergotty pyroxene, allow us to arrive at some tentative conclusions regarding the $^{40}Ar/^{36}Ar$ ratio of the "Martian interior" component. The data, if correct, have strong implications on the nature of the Martian mantle. The Chassigny meteorite has the highest relative abundance of interior versus the atmospheric component, so it would appear to be the best choice for obtaining this information. In practice, however, Chassigny is difficult because the large radiogenic contribution (due to its 1.3 Gyr crystallization age) totally dominates the ^{40}Ar budget (Ott 1988). Nevertheless, stepwise-heating data on Chassigny as well as on ALH 84001 have been interpreted as indicating for the Martian interior component a $^{40}Ar/^{36}Ar$ ratio significantly lower than that in the Martian atmosphere (Mathew and Marti 2001). The pyroxenes of our study provide us with a different and independent approach: constraining the $^{40}Ar/$

Table 4b. Decomposition of measured $^{40}Ar_{meas}$ into radiogenic $^{40}Ar_{rad}$ (Table 9a), Martian atmospheric (MA), and Martian interior (MI = rest), and inferred $^{40}Ar/^{36}Ar$ for Martian interior component.

Mineral	$^{40}Ar_{meas}$	$^{40}Ar_{rad}$	$^{129}Xe^*$	$^{40}Ar_{MA}$	$^{40}Ar_{MI}$	$(^{40}Ar/^{36}Ar)_{MI}$
Shergotty maskelynite	3.73 (0.14)	1.38 (0.44–2.30)	1.26 (0.42)	1.30 (0.43)	–	–
Shergotty pyroxene	1.60 (0.04)	0.13	0.48 (0.11)	0.49 (0.12)	1.00 (0.12)	1735 (444)
Zagami maskelynite	2.86 (0.13)	2.12 (0.69–3.54)	0.65 (0.55)	0.67 (0.56)	–	–
Zagami pyroxene	0.98 (0.04)	0.083 (0.03–0.13)	0.11 (0.09)	0.11 (0.09)	0.78 (0.10)	2822 (844)
EETA79001 pyroxene	0.52 (0.02)	0.014 (0.007–0.021)	0.29 (0.10)	0.30 (0.10)	0.21 (0.11)	–

Calculations have been performed using the "mean" radiogenic ^{40}Ar abundance; the range corresponding to various reported K abundances is given in parentheses (cf. Table 9a). Implanted Martian atmospheric $^{40}Ar_{MA}$ is inferred from $^{129}Xe^*$, where $^{129}Xe^*$ is the excess ^{129}Xe over the $^{129}Xe/^{132}$ratio = 1.03 in Chassigny (Ott 1988). An error of 0.02 has been assigned to this baseline ratio. The $^{40}Ar/^{129}Xe^*$ of the implanted Martian atmosphere = 1.03×10^6 has been taken from Bogard et al. (2001). Also shown is the inferred $^{40}Ar/^{36}Ar$ ratio of the Martian interior component (MI); a ratio $^{40}Ar/^{36}Ar = 1800$ for the Martian atmospheric component (Bogard et al. 2001) has been used for this calculation. Ar is given in units of 10^{-6} cc STP/g, Xe in 10^{-12} cc STP/g.

Table 4a. Estimation of radiogenic contributions to ^{40}Ar of mineral separates.

Mineral	$^{40}Ar_{meas}$	K (wt%)	$^{40}Ar_{rad}$	$^{40}Ar_{rad}$ (mean)
Shergotty maskelynite	3.73	0.137 (*0.066*, 0.299)[a] *0.344*[b] 0.10–0.21[c] 0.087–0.099[d]	0.92 (*0.44*, 2.01) *2.30* 0.67–1.39	1.38
Shergotty pyroxene	1.60	0.02[b]	0.13	0.13
Zagami maskelynite	2.86	0.12[e] 0.49[f] 0.095[g]	0.87 3.54 0.69	2.12
Zagami pyroxene	0.97	0.005–0.01[h] 0.0166–0.018[g]	0.035–0.090 0.12–0.13	0.08
EETA79001 pyroxene	0.70	0.001–0.002[i]	0.0071–0.021	0.014

[a]Stöffler et al. (1986): average of all given analyses (min, max); [b]Terribilini et al. (1998); [c]Smith and Hervig (1979); [d]Hale et al. (1999); [e]Stolper and McSween (1979); [f]Bogard and Garrison (1999); [g]Shih et al. 1982; [h]Treiman and Sutton (1991): range of all given analyses; [i]Steele and Smith (1982): range of all given analyses.

Estimates of radiogenic ^{40}Ar are given in units of 10^{-6} cc STP/g. They are based on various K contents as reported in the literature and radiometric ages taken the compilation by Nyquist et al. (2001): 165 ± 4 Myr (Shergotty), 177 ± 3 Myr (Zagami), and 173 ± 3 Myr (EETA79001). No loss of radiogenic Ar during the shock is assumed. Minimum and maximum values are shown in italics. The last column is the mean of maximum and minimum. They are compared to measured ^{40}Ar (column 2).

^{36}Ar ratio of the Martian interior component from mass balance considerations. Our pyroxenes have both low K and, being from shergottites, young ages so that precise knowledge about the radiogenic component is fairly uncritical.

Detailed results of our calculations, both for the pyroxenes and the maskelynite samples, are summarized in Tables 4a and 4b. Measured ^{40}Ar is assumed to be the sum of the radiogenic component ($^{40}Ar_{rad}$) from ^{40}K decay, $^{40}Ar_{MA}$ from the Martian atmosphere, and $^{40}Ar_{MI}$ from the Martian interior (with the tiny cosmogenic contribution being neglected).

$$^{40}Ar_{meas} = {}^{40}Ar_{rad} + {}^{40}Ar_{MA} + {}^{40}Ar_{MI} \quad (1)$$

while trapped ^{36}Ar (i.e., measured ^{36}Ar after subtraction of the cosmogenic fraction; listed in Table 3) is assumed to have contributions from Mars's atmosphere and interior:

$$^{36}Ar_{tr} = {}^{36}Ar_{MA} + {}^{36}Ar_{MI} \quad (2)$$

The contributions to Ar from the Martian atmospheric component listed in Table 4b are based on the observed $^{129}Xe^*$ that is a characteristic of the Martian atmospheric component ($[^{129}Xe/^{132}Xe]_{MA} = 2.6$; Bogard et al. 2001). They have been calculated as an excess over $^{129}Xe/^{132}Xe = 1.03 \pm 0.02$, the

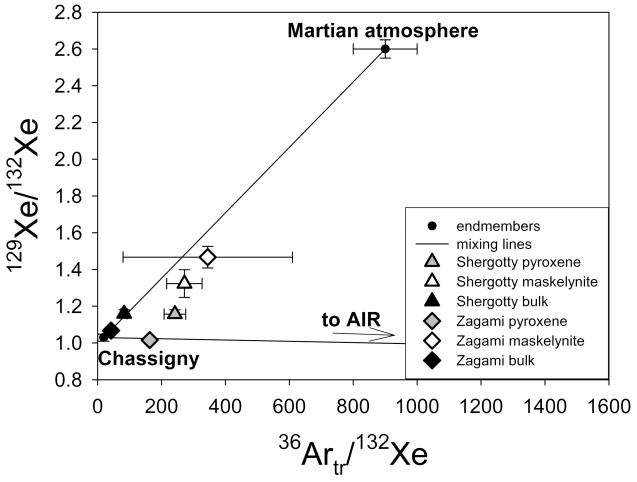

Fig. 7. $^{129}Xe/^{132}Xe$ versus $^{36}Ar/^{132}Xe$.

signature of the Martian interior component found in Chassigny (Ott 1988). Martian atmospheric $^{40}Ar_{MA}$ and $^{36}Ar_{MA}$ were derived using $^{40}Ar_{MA}/^{129}Xe^* = 1.032 \times 10^6$ and $(^{40}Ar/^{36}Ar)_{MA} = 1800$ (Bogard et al. 2001). That shock in all likelihood has introduced Martian atmosphere without fractionating the Ar/Xe ratio has been demonstrated in experiments by Bogard et al. (1986) and Wiens and Pepin (1988). No errors have been assigned to these model values; the sensitivity to the assumptions has been checked by performing them with a different set of ratios (see below).

Uncertainties are introduced into the calculation of radiogenic ^{40}Ar due to the fact that there are no "same sample" K analyses and K concentrations reported in the literature (listed in Table 4a) are quite variable. For the pyroxenes, in particular, K is low and for our separates may be even lower than those listed. This is because in many reported analyses K was below detection limit, and actually reported numbers may represent only the most K-rich cases. Fortunately, radiogenic ^{40}Ar still accounts for at most 13% of measured ^{40}Ar in Zagami pyroxene, distinctly less than that (~8%) for Shergotty pyroxene, and not more than 4% in the case of EETA79001. Gas retention ages of 165, 177, and 173 Myr were assumed for Shergotty, Zagami, and EETA79001 respectively in this calculation, together with no loss of radiogenic Ar during the shock event(s) that launched the shergottites from Mars. For the mass balance calculations in Table 4b, the mean value (without error) of the total range has been used.

Not surprisingly, the results for maskelynites and pyroxenes are quite different. For the maskelynite separates, the sum of radiogenic + trapped Martian atmospheric ^{40}Ar easily matches the measured abundances. For the pyroxenes, amounts not accounted for by these two components are ~10.0 $\times 10^{-7}$, 7.8 $\times 10^{-7}$, and 2.1 $\times 10^{-7}$ cc STP/g for Shergotty, Zagami, and EETA79001, respectively. If we assume a ~50% higher ratio $^{40}Ar_{MA}/^{129}Xe^*$, such as the ratio 1.4×10^6 inferred for EETA79001 glass by Becker and Pepin (1984a), amounts inferred for the interior component are slightly lower (8.2 $\times 10^{-7}$, 7.8 $\times 10^{-7}$, and 1.0 $\times 10^{-7}$ cc STP/g, respectively). $^{36}Ar_{MA}/^{129}Xe^*$ is virtually identical in the atmospheric sets of Bogard et al. (2001) and Becker and Pepin (1984a), so the higher $^{40}Ar_{MA}/^{129}Xe^*$ in the latter directly corresponds to their higher inferred $(^{40}Ar/^{36}Ar)_{MA}$ of ~2400 instead of ~1800. A possible explanation for at least part of the difference is that Becker and Pepin (1984a) arrived at their estimate by subtracting from the gases measured in their EETA79001 glass sample those measured in a lithology A sample, without taking into account the higher K and hence radiogenic Ar content of the glass. In any case, using the extreme value of Becker and Pepin leads to a higher contribution to ^{40}Ar from Mars atmosphere and an accordingly reduced contribution from the interior. With essentially no effect on ^{36}Ar, this difference then also directly translates into the inferred $^{40}Ar/^{36}Ar$ ratio for the interior component. For our best case (analytically), Shergotty pyroxene, our data yield values of 1735 ± 444 (Table 4b) using Bogard et al. (2001) versus 1429 ± 456 using Becker and Pepin (1984a).

As discussed earlier, the radiogenic contribution to ^{40}Ar in Shergotty pyroxene is 8% at most, so the uncertainty introduced by this is much smaller than the difference between using the two estimates for the Martian atmosphere. In fact, in our calculations the main uncertainties in the Shergotty pyroxene $(^{40}Ar/^{36}Ar)_{MI}$ ratio are introduced about equally from both the error in the $^{36}Ar_{tr}$ (MA +MI) abundance due to the uncertainty assigned to the endmember compositions in correcting for cosmogenic Ar (cf. Table 3) and the analytical error in excess ^{129}Xe that is used as a proxy for the atmospheric contribution (Table 4b). Barring the presence of additional components not taken into account, it seems safe to conclude that Martian interior Ar in Shergotty pyroxene has a high $^{40}Ar/^{36}Ar$ ratio of ~2000, similar to that in the atmosphere. Of course, in a qualitative way, this also follows directly from considering that a) measured ratios $^{40}Ar/^{36}Ar_{tr}$ (Table 3) are similar to $^{40}Ar/^{36}Ar$ in the Martian atmosphere, b) radiogenic contributions are small, and c) contributions from the interior component are of similar size as those from the atmospheric component (Fig. 7). The Shergotty pyroxene result is confirmed, although with less precision, by our Zagami pyroxene data (Table 4b). No conclusions can be drawn from the data for EETA79001 pyroxene because abundances are so low that the remaining Ar (both ^{36}Ar and ^{40}Ar) (Tables A3, 3, and 4b) that can be attributed to the interior source is dwarfed by the analytical errors.

The value $(^{40}Ar/^{36}Ar)$ derived here is clearly different from values for Ar in Mars interior derived by others so far. Bogard and Garrison (1999) conclude from shergottite analyses that the ratio for the Martian mantle component "is probably <500 but is poorly constrained." For the EETV component in EETA79001, which may be related to the

Martian interior, Wiens (1988) reports a possible range of 430 to 680. Low $^{40}Ar/^{36}Ar$ ratios were also measured by Mathew and Marti (2001) in both Chassigny (212 ± 12) and in ALH 84001 (128 ± 6) in the gas released at the highest extraction temperature of 1600° C and were attributed to Martian interior argon.

However, there are potential problems associated with all of these results. As for the shergottites, Bogard and Garrison (1999) estimate an approximate upper limit of ~330 from intermediate temperature steps for ALHA77005 and ~300 from Shergotty, but themselves recognize that the situation is somewhat problematic and air contamination cannot be completely ruled out. On the other hand, the low ratios for Chassigny and ALH 84001 were measured on small amounts of gas released at the highest extraction temperature. The same is true for the only one of our analyses listed in Table 3 (the 1700 °C step of Shergotty pyroxene, which does not contribute significantly to the total) showing a low $^{40}Ar/^{36}Ar_{tr}$ ratio. We consider an underestimated blank the most likely explanation. The mass balance approach, finally, could be compromised in two ways: first, if the pyroxenes were not completely degassed at the time of their formation ~170 Myr ago, but inherited some radiogenic Ar, and and second, if additional components not considered in our mass balance calculations were present. As for incomplete degassing, Bogard and Garrison (1999) discuss the possibility that inherited radiogenic Ar is present in Zagami feldspar leading to a somewhat (~15%) enhanced apparent Ar-Ar age of 209 Myr. Presence of significant amounts of inherited radiogenic Ar in our pyroxenes appears unlikely, however. For one, the similarity of the interior with the atmospheric isotopic ratio, while possible, would be a remarkable coincidence. Note further that for our Shergotty and Zagami pyroxenes the interior component as listed in Table 4b dominates the ^{40}Ar inventory and an ~15% higher radiogenic contribution would be negligible. Even an addition to pyroxene of 15% of the radiogenic ^{40}Ar concentration measured in maskelynite, difficult because of mass balance considerations alone already, would not bring down our inferred $(^{40}Ar/^{36}Ar)_{MI}$ into the range below ~1000. As for additional components, the fact that the pyroxene data do not plot on the Chassigny-Mars atmosphere mixing line in Fig. 7 may be taken as evidence for this. Alternatively, this could be due to incomplete degassing of Xe from our pyroxenes. However, there is no evidence for this; an upper limit to the amount of ^{132}Xe released at the 1700 °C step not listed in detail in Table A is 0.23 $\times 10^{-12}$ cc STP/g (~6% of the total given) (Schwenzer 2004). Even so, if we correct for such an effect by moving the data points in Fig. 7 upward and/or to the left so that they fall on the mixing line—corresponding to increasing the ratio of Martian atmospheric $^{129}Xe^*$ to trapped ^{36}Ar—$(^{40}Ar/^{36}Ar)_{MI}$ ratios calculated in our approach are still high. If an extra component is present in Ar (and Kr) (Fig. 8), our conclusion that $^{40}Ar/^{36}Ar$ is high applies to the sum of Martian interior Ar and that of the

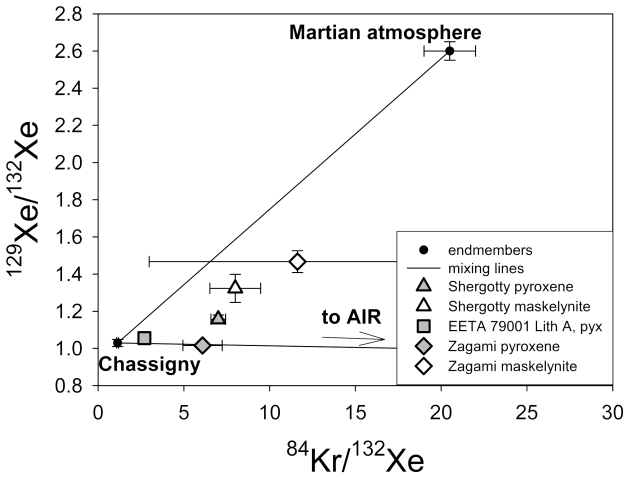

Fig. 8. $^{129}Xe/^{132}Xe$ versus $^{84}Kr/^{132}Xe$.

putative extra component. On the other hand, without further understanding of the trapping process, there is no obvious reason why the elemental composition of the interior component in Shergotty pyroxenes should be exactly equal to that in Chassigny (olivine). In support of this, data points for pyroxenes and maskelynites fall on mixing lines in Figs. 7 and 8, joining Martian atmosphere with a composition $^{36}Ar/^{132}Xe$ ~180, $^{84}Kr/^{132}Xe$ ~6. The presence of important additional gas carriers besides pyroxene and maskelynite that may shift the meteorites' totals to the MA-Chassigny mixing line is further indicated by the fact that they account for no more than 20–30% of $^{129}Xe^*$, but most (~93% for Shergotty and 66% for Zagami) of the meteorites' ^{40}Ar.

Taking all data (literature as well as ours) at face value, the observed/inferred differences in $(^{40}Ar/^{36}Ar)_{MI}$ point to the possibility of variability (as function of locality and/or time) in the Ar inventory of the mantle source(s) from which the different petrologic groups of Martian meteorites acquired their "interior" noble gas component. In a way, this would be similar to the case of Xe, where in Chassigny two different "interior components," Chass-S and Chass-E, have been identified (Mathew and Marti 2001). If confirmed, this will put new and interesting constraints on the geological development of planet Mars.

SUMMARY

1. We obtained cosmic-ray exposure ages for Shergotty (2.48 Myr), Zagami (2.73 Myr), and EETA79001 (lith. A) (0.65 Myr).
2. K-Ar ages cannot be calculated due to gain, redistribution, and loss of Ar caused by shock metamorphism.
3. Shock metamorphism caused significant loss of radiogenic ^{4}He: ~70% for Shergotty, ~47% for Zagami, and ~56% for EETA79001 (lith. A).

4. The Ar degassing patterns suggest the implanted ^{40}Ar tends to degas before the melting temperature of the phase, whereas ^{36}Ar and ^{38}Ar, which are primarily located in the mineral structure, tend to degas at higher temperatures. In contrast to ^{4}He, which has been lost due to shock effects and where the extent of loss can be related to the degree of shock metamorphism, ^{40}Ar from the Martian atmosphere is implanted by the same process (shock) that caused loss of radiogenic ^{40}Ar.
5. For neon, in addition to the results for the mineral separates of this study, we discuss bulk meteorite data from 13 Martian meteorites of all subgroups. Data on production rates for galactic cosmic ray exposure (Leya et al. 2000) provide us with a tool to eliminate variation of the cosmogenic $(^{21}Ne/^{22}Ne)_c$ ratio due to chemistry and thus to identify contributions from solar cosmic rays. The mineral separate results confirm the results based on bulk data: there is no evidence for solar cosmic-ray effects in case of Chassigny, ALH 84001, and the nakhlites, whereas it is required for all of the shergottites.
6. Maskelynite shows the highest abundance and contains a major fraction of the Martian atmospheric gas, but Martian gas both from the atmosphere and from the interior is also found in pyroxene.
7. By subtracting from measured Ar radiogenic contributions (minor in the case of the pyroxenes) as well as implanted Martian atmosphere (derived via the characteristic excess ^{129}Xe), we derive an estimate for the Martian interior $(^{40}Ar/^{36}Ar)_{MI}$ ratio in the shergottites. Barring the presence of additional components, the ratio is ~2000, similar to the composition of the atmospheric component, which is in stark contrast to estimates for Chassigny and ALH 84001. This may reflect the temporal development of the Martian interior, but may also point to an inhomogeneous Martian interior with different volatile reservoirs sampled by the different groups of Martian meteorites.

Acknowledgments–We are grateful to the Johnson Space Center (Houston, Texas, USA), the Museum of Natural History (London), and the Museum für Naturkunde (Berlin) for providing samples of EETA79001, Shergotty, and Zagami, respectively. We thank Ansgar Greshake (Museum für Naturkunde, Berlin) and his group, especially Jörg Fritz and Jana Berlin, for handpicking the mineral separates. Thanks to Allan H. Treiman (LPI, Houston, Texas, USA), who provided the best estimate for bulk rock chemistry of Lafayette, and Ingo Leya (University of Bern, Switzerland), who donated his spreadsheets for the neon calculation (so we could avoid hours and hours of typing). We very much appreciate constructive reviews by D. D. Bogard and O. Eugster and Associate Editor T. D. Swindle. This work was funded in part by the German Science Foundation.

Editorial Handling—Dr. Timothy Swindle

REFERENCES

Alexeev V. A. 1998. Parent bodies on L and H chondrites: Times of catastrophic events. *Meteoritics & Planetary Science* 33:145–152.

Alexeev V. A. 2005. The history of ordinary chondrites from the data on stable isotopes of noble gases (a review). *Solar System Research* 39:124–149.

Artemieva N. A. and Ivanov B. 2004. Launch of Martian meteorites in oblique impacts. *Icarus* 171:84–101.

Bastian T. 2003. Radiochemische Analyse langlebiger kosmogener Radionuklide in Marsmeteoriten und Chondriten: Wirkungquerschnitte, Produktionsraten und Modellrechnungen. Ph. D. thesis, Mathematisch-Naturwissenschaftliche Fakultät der Universität zu Köln, Köln, Germany.

Beck P., Gillet Ph., El Goresy A., and Moustefaoui S. 2005. Timescales of shock processes in chondritic and Martian meteorites. *Nature* 435:1071–1074.

Becker R. H. and Pepin R. O. 1984a. The case for a Martian origin of the shergottites: Nitrogen and noble gases in EETA79001. *Earth and Planetary Science Letters* 69:225–242.

Becker R. H. and Pepin R. O. 1984b. Remeasurement of nitrogen in EETA79001 glass. *Meteoritics* 19:336–337.

Becker R. H. and Pepin R. O. 1986. Nitrogen and light noble gases in Shergotty. *Geochimica et Cosmochimica Acta* 50:993–1000.

Boctor N. Z., Meyer H. O. A., and Kullerud G. 1976. Lafayette meteorite: Petrology and opaque mineralogy. *Earth and Planetary Science Letters* 32:69–76.

Bogard D. 1982. Trapped noble gases in EETA79001 shergottite. *Meteoritics* 17:185–186.

Bogard D. D. 1997. A reappraisal of the Martian $^{36}Ar/^{38}Ar$ ratio. *Journal of Geophysical Research* 102:1653–1661.

Bogard D. D. and Garrison D. H. 1998. Relative abundances of argon, krypton, and xenon in the Martian atmosphere as measured in Martian meteorites. *Geochimica et Cosmochimica Acta* 62:1829–1835.

Bogard D. D. and Garrison D. H. 1999. Argon-39-argon-40 "ages" and trapped argon in Martian shergottites, Chassigny, and Allan Hills 84001. *Meteoritics & Planetary Science* 34:451–473.

Bogard D. D. and Johnson P. 1983. Martian gases in an Antarctic meteorite? *Science* 221:651–654.

Bogard D. D., Huneke J. C., Burnett D. S., and Wasserburg G. J. 1971. Xe and Kr analyses of silicate inclusions from iron meteorites. *Geochimica et Cosmochimica Acta* 35:1231–1254.

Bogard D. D., Nyquist L. E., and Johnson P. 1984. Noble gas contents of shergottites and implications for the Martian origin of SNC meteorites. *Geochimica et Cosmochimica Acta* 48:1723–1739.

Bogard D. D., Hörz F., and Johnson P. 1986. Shock-implanted noble gases: An experimental study with implications for the origin of Martian gases in shergottite meteorites. Proceedings, 17th Lunar and Planetary Science Conference. pp. 99–114.

Bogard D. D., Clayton R. N., Marti K., Owen T., and Turner G. 2001. Martian volatiles: Isotopic composition, origin, and evolution. *Space Science Reviews* 96:425–458.

Clayton R. N. and Mayeda T. K. 1983. Oxygen isotopes in eucrites, shergottites, nakhlites, and chassignites. *Earth and Planetary Science Letters* 62:1–6.

Deer W. A., Howie R. A., and Zusman J. 1992. *An introduction to rock-forming minerals.* Harlow, UK: Longman. 696 p.

Dreibus G., Spettel B., Haubold R., Jochum K.-P., Palme H., Wolf D., and Zipfel J. 2000. Chemistry of a new shergottite: Sayh al Uhaymir 005 (abstract). *Meteoritics & Planetary Science* 35:A49.

El Goresy A., Dubrovinsky L., Sharp T. G., and Chen M. 2004. Stishovite and post-stishovite polymorphs of silica in the shergotty meteorite: Their nature, petrographic settings versus theoretical predictions and relevance to the Earth's mantle. *Journal of Physics and Chemistry of Solids* 65:1597–1608.

Eugster O. 1988. Cosmic-ray production rates for ^{3}He, ^{21}Ne, ^{38}Ar, ^{83}Kr, and ^{126}Xe in chondrites based on ^{81}Kr-Kr exposure ages. *Geochimica et Cosmochimica Acta* 52:1649–1662.

Eugster O. and Michel Th. 1995. Common asteroid break-up events of eucrites, diogenites, and howardites and cosmic-ray production of noble gases in achondrites. *Geochimica et Cosmochimica Acta* 59:177–199.

Eugster O., Weigel A., and Polnau E. 1996. Two different ejection events for basaltic shergottites QUE 94201, Zagami and Shergotty (2.6 Ma ago) and lherzolithic shergottites LEW 88516 and ALH 77005 (3.5 Ma ago). Proceedings, 27th Lunar and Planetary Science Conference. pp. 345–346.

Eugster O., Weigel A., and Polnau E. 1997. Ejection times of Martian meteorites. *Geochimica et Cosmochimica Acta* 61:2749–2757.

Eugster O., Busemann H., Lorenzetti S., and Terriblini D. 2002. Ejection ages from krypton-81-krypton-83 dating and pre-atmospheric sizes of Martian meteorites. *Meteoritics & Planetary Science* 37:1345–1360.

Freundel M., Schultz L., and Reedy R. C. 1986. Terrestrial ^{81}Kr-Kr ages of Antarctic meteorites. *Geochimica et Cosmochimica Acta* 50:2663–2673.

Fritz J. 2005. Aufbruch vom Mars; Petrologie und Stosswellenmetamorphose von Marsmeteoriten. Ph.D. thesis, Humboldt-Universität zu Berlin, Berlin, Germany.

Fritz J., Greshake A., and Stöffler D. 2003. Launch conditions for Martian meteorites: Plagioclase as a shock pressure barometer (abstract #1335). 34th Lunar and Planetary Science Conference. CD-ROM.

Fritz J., Artemieva N., and Greshake A. 2005. Ejection of Martian meteorites. *Meteoritics & Planetary Science* 40:1393–1411.

Garrison D. H. and Bogard D. D. 1998. Isotopic composition of trapped and cosmogenic noble gases in several Martian meteorites. *Meteoritics & Planetary Science* 33:721–736.

Garrison D. H., Rao M. N., and Bogard D. D. 1995. Solar-proton-produced neon in shergottite meteorites and implications for their origin. *Meteoritics* 30:738–747.

Gilmour J. D., Whithby J. A., and Turner G. 2001. Disentangling xenon components in Nakhla: Martian atmosphere, spallation and Martian interior. *Geochimica et Cosmochimica Acta* 65:343–354.

Gladman B. 1997. Destination: Earth. Martian meteorite delivery. *Icarus* 130:228–246.

Gladman B. J., Burns J. A., Duncan M., Lee P., and Levison H. F. 1996. The exchange of impact ejecta between terrestrial planets. *Science* 271:1387–1392.

Goodrich C. A. 2002. Olivine-phyric Martian basalts: A new type of shergottite. *Meteoritics & Planetary Science* 37:B31–B34.

Grady M. M., Wright I. P., and Pillinger C. T. 1997. A carbon and nitrogen isotope study of Zagami. *Journal of Geophysical Research* 102:9165–9173.

Graf T., Baur H., and Signer P. 1990. A model for the production of cosmogenic nuclides in chondrites. *Geochimica et Cosmochimica Acta* 54:2521–2534.

Hale V. P. S., McSween H. Y., Jr., and McKay G. A. 1999. Re-evaluation of intercumulus liquid composition and oxidation state for the Shergotty meteorite. *Geochimica et Cosmochimica Acta* 63:1459–1470.

Heymann D. 1967. On the origin of hypersthene chondrites: Ages and shock effects of black chondrites. *Icarus* 6:189–221.

Hohenberg C. M., Marti K., Podosek F. A., Reedy R. C., and Shirck J. R. 1978. Comparisons between observed and predicted cosmogenic noble gases in lunar samples. Proceedings, 9th Lunar Science Conference. pp. 2311–2344.

Hohenberg C. M., Hudson B., Kennedy B. M., and Podosek F. A. 1981. Xenon spallation systematics in Angra dos Reis. *Geochimica et Cosmochimica Acta* 45:1909–1915.

Jochum K. P., Stoll B., Amini M., and Palme H. 2001. Limited trace element fractionation in SNC meteorites (abstract). *Meteoritics & Planetary Science* 36:A90–A91.

Kim K. J., Masarik J., and Reedy R. C. 2005. The effects of geometry on nuclide production processes in meteorites (abstract). *Meteoritics & Planetary Science* 40:A80.

Krasnopolsky V. A., Bowyer S., Chakrabarti S., Gladstone G. R., and McDonald J. S. 1994. First measurement of helium on Mars: Implications for the problem of radiogenic gases on the terrestrial planets. *Icarus* 109:337–351.

Kring E. A., Gleason J. D., Swindle T. D., Nishiizumi K., Caffee M. W., Hill D. H., Jull A. J. T., and Boynton W. V. 2003. Composition of the first bulk melt sample from a volcanic region of Mars: Queen Alexandra Range 94201. *Meteoritics & Planetary Science* 38:1833–1848.

Leya I., Lange H.-J., Neumann S., Wieler R., and Michel R. 2000. The production of cosmogenic nuclides in stony meteoroids by galactic cosmic-ray particles. *Meteoritics & Planetary Science* 35:259–286.

Lodders K. 1998. A survey of shergottite, nakhlite, and chassigny meteorites whole-rock compositions. *Meteoritics & Planetary Science* 33:A183–A190.

Malavergne V., Guyot F., Benzerara K., and Martinez I. 2001. Description of new shock-induced phases in the Shergotty, Zagami, Nakhla, and Chassigny meteorites. *Meteoritics & Planetary Science* 36:1297–1305.

Marti K., Kim J. S., Thakur A. N., McCoy T. J., and Keil K. 1995. Signatures of the Martian atmosphere in glass of the Zagami meteorite. *Science* 267:1981–1984.

Mathew K. J. and Marti K. 2001. Early evolution on Martian volatiles: Nitrogen and noble gas components in ALH 84001 and Chassigny. *Journal of Geophysical Research* 106:1401–1422.

Mathew K. J., Kim J. S., and Marti K. 1998. Martian atmospheric and indigenous components of xenon and nitrogen in the Shergotty, Nakhla, and Chassigny group meteorites. *Meteoritics & Planetary Science* 33:655–664.

McSween H. Y., Jr. 1984. SNC meteorites: Are they Martian rocks? *Geology* 12:3–6.

McSween H. Y., Jr. 1994. What we have learned about Mars from SNC meteorites. *Meteoritics* 29:757–779.

McSween H. Y., Jr. 2002. The rocks of Mars, from far and near. *Meteoritics & Planetary Science* 37:7–25.

McSween H. Y., Jr. and Stolper E. M. 1980. Basaltic meteorites. *Scientific American* 242:44–53.

Meyer C. 2003. *Mars Meteorite Compendium 2001*. Houston, Texas: National Aeronautics and Space Administration. 371 p.

Mohapatra R. K. 2004. Understanding Mars from meteorites—The nitrogen and noble gas perspective. *Current Science* 86:1499–1505.

Mohapatra R. K., Mahajan R. R., and Murty S. V. S. 1998. Nitrogen and argon in Shergotty. *Meteoritics & Planetary Science* 33: A112.

Mohapatra R. K., Schwenzer S. P., and Ott U. 2003. Trapped neon in the Martian meteorite SaU 005 (abstract). *Meteoritics & Planetary Science* 38:A109.

Müller H. W. and Zähringer J. 1969. Rare gases in stony meteorites.

In *Meteorite research,* edited by Millman P. M. Dordrecht, The Netherlands: Kluwer. pp. 845–856.

Niedermann S. and Eugster O. 1992. Noble gases in lunar anorthositic rocks 60018 and 65315: Acquisition of terrestrial krypton and xenon indicating an irreversible adsorption process. *Geochimica et Cosmochimica Acta* 56:493–509.

Niemeyer S. and Leich D. A. 1976. Atmospheric rare gases in lunar rock 60015. Proceedings, 7th Lunar Science Conference. pp. 587–597.

Nier A. O., Hanson W. B., Seiff A., McElroy M. B., Spencer N. W., Duckett R. J., Knight T. C. D., and Cook W. S. 1976. Composition and structure of the Martian atmosphere: Preliminary results from Viking 1. *Science* 193:786–788.

Nyquist L. E., Bogard D. D., Shih C.-Y., Greshake A., Stöffler D., and Eugster O. 2001. Ages and geologic histories of Martian meteorites. *Space Science Reviews* 96:105–164.

Ocker K. D. and Gilmour J. D. 2004. Martian xenon components in Shergotty mineral separates: Locations, sources, and trapping mechanisms. *Meteoritics & Planetary Science* 39:1967–1981.

Ott U. 1988. Noble gases in SNC meteorites: Shergotty, Nakhla, Chassigny. *Geochimica et Cosmochimica Acta* 52:1937–1948.

Ott U. 2002. Noble gases in meteorites—Trapped components. In *Noble gases in geochemistry and cosmochemistry,* edited by Porcelli D., Ballentine C. J., and Wieler R. Washington, D.C.: Mineralogical Society of America. pp. 71–100.

Ott U. and Begemann F. 1985. Are all "Martian" meteorites from Mars? *Nature* 317:509–512.

Ott U. and Löhr H. P. 1992. Noble gases in the new shergottite LEW 88516 (abstract). *Meteoritics* 27:271.

Ott U., Löhr H. P., and Begemann F. 1988. New noble gas data for SNC meteorites: Zagami, Lafayette, and etched Nakhla (abstract). *Meteoritics* 23:295–296.

Ott U., Löhr H. P., and Begemann F. 1996. Etching and crushing SNCs: More noble gas data (abstract). *Meteoritics & Planetary Science* 31:A103.

Owen T., Biemann K., Rushneck D. R., Biller J. E., Howarth D. W., and Lafleur A. L. 1977. The composition of the atmosphere at the surface of Mars. *Journal of Geophysical Research* 82:4635–4639.

Ozima M. and Podosek F. A. 2002. *Noble gas geochemistry.* Cambridge: Cambridge University Press. 286 p.

Park J. and Nagao K. 2006. New insights on Martian atmospheric neon from Martian meteorite, Dhofar 378 (abstract #1110). 37th Lunar and Planetary Science Conference. CD-ROM.

Park J., Okazaki R., and Nagao K. 2001. Noble gases in SNC meteorites: Dar al Gani 489, Sayh al Uhaymir 005, and Dhofar 019 (abstract). *Meteoritics & Planetary Science* 36:A121–A122.

Pepin R. O. 1991. On the origin and early evolution of terrestrial planet atmospheres and meteoritic volatiles. *Icarus* 92:2–79.

Rao M. N., Garrison D. H., Bogard D. D., and Reedy R. C. 1994. Determination of the flux and energy distribution of energetic solar protons in the past 2 Myr using lunar rock 68815. *Geochimica et Cosmochimica Acta* 58:4231–4245.

Reedy R. C. 1992. Solar-proton production of neon and argon (abstract). 23rd Lunar and Planetary Science Conference. pp. 1133–1134.

Rieder R., Gellert R., Anderson R. C., Brückner J., Clark B. C., Dreibus G., Economou T., Klingelhöfer G., Lugmair G. W., Ming D. W., Squyres S. W., d'Uston C., Wänke H., Yen A., and Zipfel J. 2004. Chemistry of rocks and soils at Meridiani Planum from the Alpha Particle X-ray Spectrometer. *Science* 306:1746–1749.

Russell S. S., Zipfel J., Grossman J. N., and Grady M. M. 2002. The Meteoritical Bulletin, No. 86. *Meteoritics & Planetary Science* 37:A157–A184.

Russell S. S., Zipfel J., Folco L., Jones R., Grady M. M., McCoy T., and Grossman J. N. 2003. The Meteoritical Bulletin, No. 87. *Meteoritics & Planetary Science* 38:A189–A248.

Russell S. S., Folco L., Grady M. M., Zolensky M. E., Jones R., Righter K., Zipfel J. R., and Grossman J. N. 2004. The Meteoritical Bulletin, No. 88. *Meteoritics & Planetary Science* 39:A215–A272.

Schultz L. and Franke L. 2004. Helium, neon, and argon in meteorites. A data collection. *Meteoritics & Planetary Science* 39:1889–1890.

Schultz L., Franke L., and Bevan A. W. R. 2005. Noble gases in ten Nullarbor chondrites: Exposure ages, terrestrial ages, and weathering effects. *Meteoritics & Planetary Science* 40:659–664.

Schwenzer S. P. 2004. Marsmeteorite: Edelgase in Mineralseparaten, Gesamtgesteinen und terrestrischen Karbonaten. Ph.D. thesis, Johannes Gutenberg-Universität Mainz, Mainz, Germany.

Schwenzer S. P., Fritz J., Greshake A., Herrmann S., Jochum K. P., Ott U., Stöffler D., and Stoll B. 2004. Helium loss and shock pressure in Martian meteorites—A relationship (abstract). *Meteoritics & Planetary Science* 39:A96.

Schwenzer S. P., Herrmann S., and Ott U. 2005. Noble gases in mineral separates from Shergotty and Zagami (abstract # 1310). 36th Lunar and Planetary Science Conference. CD-ROM.

Shih C.-Y., Nyquist L. E., Bogard D. D., McKay G. A., Wooden J. L., Bansal B. M., and Wiesmann H. 1982. Chronology and petrogenesis of young achondrites, Shergotty, Zagami, and ALHA77005: Late magmatism on a geologically active planet. *Geochimica et Cosmochimica Acta* 46:2323–2344.

Smith S. P. and Huneke J. C. 1975. Cosmogenic neon produced from sodium in meteoritic minerals. *Earth and Planetary Science Letters* 36:359–362.

Smith J. V. and Hervig R. L. 1979. Shergotty meteorite: Mineralogy, petrography, and minor elements. *Meteoritics* 14: 121–142.

Srinivasan B., Lewis R. S., and Anders E. 1978. Noble gases in Allende and Abee meteorites and a gas-rich mineral fraction: Investigation by stepwise heating. *Geochimica et Cosmochimica Acta* 42:183–198.

Stauffer H. 1962. On the production of rare gas isotopes in stone meteorites. *Journal of Geophysical Research* 67:2023–2028.

Steele I. M. and Smith J. V. 1982. Petrography and mineralogy of two basalts and olivine-pyroxene-spinel fragments in achondrite EETA79001. Proceedings, 13th Lunar and Planetary Science Conference. pp. A375–A384.

Stöffler D., Ostertag R., Jammes C., Pfannschmidt G., Sen Gupta P. R., Simon S. B., Papike J. J., and Beauchamp R. H. 1986. Shock metamorphism and petrography of the Shergotty achondrite. *Geochimica et Cosmochimica Acta* 50:889–903.

Stolper E. M. and McSween H. Y., Jr. 1979. Petrology and origin of the shergottite meteorites. *Geochimica et Cosmochimica Acta* 43:1475–1498.

Swindle T. D. 2002. Martian noble gases. In *Noble gases in geochemistry and cosmochemistry,* edited by Porcelli D., Ballentine C. J., and Wieler R. Washington, D.C.: Mineralogical Society of America. pp. 171–190.

Swindle T. D., Caffee M. W., and Hohenberg C. M. 1986. Xenon and other noble gases in shergottites. *Geochimica et Cosmochimica Acta* 50:1001–1015.

Terribilini D., Eugster O., Burger M., Jakob A., and Krähenbühl U. 1998. Noble gases and chemical composition of Shergotty mineral fractions, Chassigny, and Yamato-793605: The trapped argon-40/argon-36 ratio and ejection times of Martian meteorites. *Meteoritics & Planetary Science* 33:677–684.

Treiman A. H. 2005. The nakhlite meteorites: Augite-rich igneous rocks from Mars. *Chemie der Erde* 65:203–270.

Treiman A. H. and Sutton S. R. 1991. Zagami: Trace-element zoning of pyroxenes by synchrotron X-ray (SXRF) microprobe, and implications for rock genesis (abstract). 22nd Lunar and Planetary Science Conference. pp. 1411–1412.

Tschermak M. G. 1872. Die Meteorite von Shergotty und Gopalpur. *Sitzungsberichte der Mathematisch-naturwissenschaftlichen Classe, Akademie der Wissenschaften Wie*n 65:122–146.

Tschermak M. G. 1883. Beitrag zur Classification der Meteorite. *Sitzungsberichte der Mathematisch-naturwissenschaftlichen Classe, Akademie der Wissenschaften Wien* 88:347–371.

Wänke H. 1966. Meteoritenalter und verwandte Probleme der Kosmochemie. *Fortschritte der Chemie* 7:322–408.

Wasson J. T. and Wetherill G. W. 1979. Dynamical chemical and isotopic evidence regarding the formation locations of asteroids and meteorites. In *Asteroids,* edited by Gehrels T. Tucson, Arizona: The University of Arizona Press. pp. 926–974.

Wetherill G. W. and Chapman C. R. 1988. Asteroids and meteoroids. In *Meteorites and the early solar system,* edited by Kerridge J. F. and Matthews M. S. Tucson, Arizona: The University of Arizona Press. pp. 35–67.

Wieler R. 2002. Cosmic-ray-produced noble gases in meteorites. In *Noble gases in geochemistry and cosmochemistry,* edited by Porcelli D., Ballentine C. J., and Wieler R. Washington, D.C.: Mineralogical Society of America. pp. 125–170.

Wiens R. C. 1988. Noble gases released by vacuum crushing of EETA79001 glass. *Earth and Planetary Science Letters* 91:55–65.

Wiens R. C. and Pepin R. O. 1988. Laboratory shock emplacement of noble gases, nitrogen, and carbon dioxide into basalt, and implications for trapped gases in shergottite EETA79001. *Geochimica et Cosmochimica Acta* 52:295–307.

Wiens R. C., Becker R. H., and Pepin R. O. 1986. The case for a Martian origin of the shergottites II. Trapped and indigenous gas components in EETA79001 glass. *Earth and Planetary Science Letters* 77:149–158.

Wood C. A. and Ashwal L. D. 1981. SNC meteorites: Igneous rocks from Mars? Proceedings, 12th Lunar and Planetary Science Conference. pp. 1359–1375.

Wright I. P., Grady M. M., and Pillinger C. T. 1988. Carbon, oxygen, and nitrogen isotopic composition of possible Martian weathering products in EETA7001. *Geochimica et Cosmochimica Acta* 52:917–924.

Zipfel J., Scherer P., Spettel B., Dreibus G., and Schultz L. 2000. Petrology and chemistry of the new shergottite Dar al Gani 476. *Meteoritics & Planetary Science* 35:95–106.

APPENDIX

Table A1. Noble gas and nitrogen measurements on EETA79001, Shergotty, and Zagami reported in the literature. For He, Ne, and Ar data see also the data collection of Schultz and Franke (2004). Conc. = elemental concentrations reported; isot. = isotopic ratios reported.

		He		Ne		Ar		Kr		Xe		N_2	
Reference	Author's sample name	Conc.	Isot.	Conc.	Isot.	Conc.	Isot.	Conc.	Isot.	Conc.	Isot.	Conc.	Isot.
EETA79001													
Bogard et al. (1984)	,34 lith-a wr	✓	✓	✓	✓	✓	✓	✓		✓			
	,92 lith-a wr	✓	✓	✓	✓	✓	✓	✓		✓			
	,127 lith-a wr	✓	✓	✓	✓	✓	✓	✓		✓			
	,130 lith-a wr	✓	✓	✓	✓	✓	✓	✓		✓			
	,133 lith-a wr	✓	✓	✓	✓	✓	✓	✓		✓			
	,136 lith-a wr	✓	✓	✓	✓			✓		✓			
	,42 lith-b wr#1	✓	✓	✓	✓	✓	✓	✓		✓			
	,42 lith-b wr#2	✓	✓	✓	✓	✓	✓	✓		✓			
	,42 lith-b plag	✓	✓	✓	✓	✓	✓	✓		✓			
	,27 glass	✓	✓	✓	✓	✓	✓	✓		✓			
	,54 glass	✓	✓	✓	✓	✓	✓	✓		✓			
Becker and Pepin (1984a)	,34 A#2	✓	✓	✓	✓	✓	✓	✓	✓	✓	✓	✓	✓
	,27 C#2	✓	✓	✓	✓	✓	✓	✓	✓	✓	✓	✓	✓
Becker and Pepin (1984b)	Glass											✓	✓
Wiens et al. (1986)	,22 C#3	✓	✓		✓		✓					✓	✓
Swindle et al. (1986)	Lith. A, EETA79001, 58			✓	✓	✓	✓						
	Lith. C, EETA79001, 122			✓	✓	✓	✓	✓	✓	✓	✓		
Becker and Pepin (1986)	,59 ,116	✓	✓	✓	✓	✓	✓					✓	✓
Wiens (1988)	,245	✓	✓	✓	✓	✓	✓	✓	✓	✓	✓		
Wright et al. (1988)	,239											✓	✓
Mathew et al. (1998)	,1 glass									✓	✓	✓	✓
Bogard and Garrison (1998); Garrison and Bogard (1998)	8A, glass	✓	✓	✓	✓	✓	✓	✓	✓	✓	✓		
	8B, glass	✓	✓	✓	✓	✓	✓	✓	✓	✓	✓		
	104, glass	✓	✓	✓	✓	✓	✓	✓	✓	✓	✓		
Shergotty													
Stauffer (1962)	Shergotty	(✓)		✓		✓	✓						
Müller and Zähringer (1969)	Shergotty	✓	✓	✓	✓	✓	✓	✓		✓			
Becker and Pepin (1986)	,8	✓	✓	✓	✓	✓	✓					✓	✓
	,21	✓	✓	✓	✓	✓	✓					✓	✓
Swindle et al. (1986)	Shergotty									✓	✓		
Ott and Begemann (1985); Ott (1988)	KP3	✓	✓	✓	✓	✓	✓	✓	✓	✓	✓		
	SIII/IV	✓	✓	✓	✓	✓	✓	✓	✓	✓	✓		
Bogard and Garrison (1998); Garrison and Bogard (1998)	B, glass	✓	✓	✓	✓	✓	✓	✓	✓	✓	✓		
	A, whole rock	✓	✓	✓	✓	✓	✓	✓	✓	✓	✓		
Mohapatra et al. (1998)	Shergotty					✓	✓					✓	✓
Terribilini et al. (1998)	Bulk	✓	✓	✓	✓	✓	✓						

Table A1. *Continued.* Noble gas and nitrogen measurements on EETA79001, Shergotty, and Zagami reported in the literature. For He, Ne, and Ar data see also the data collection of Schultz and Franke (2004). Conc. = elemental concentrations reported; isot. = isotopic ratios reported.

		He		Ne		Ar		Kr		Xe		N_2	
Reference	Author's sample name	Conc.	Isot.	Conc.	Isot.	Conc.	Isot.	Conc.	Isot.	Conc.	Isot.	Conc.	Isot.
	Pyroxene	✓	✓	✓	✓	✓	✓						
	Maskelynite/mesostasis	✓	✓	✓	✓	✓	✓						
Ocker and Gilmour (2004)	Whole rock									✓	✓		
	Maskelynite-dominated minerals separates									✓	✓		
	Opaque-dominated minerals separates									✓	✓		
	Pyroxene-dominated minerals separates									✓	✓		
Zagami													
Bogard et al. (1984)	wr	✓	✓	✓	✓	✓	✓	✓		✓			
Ott et al. (1988)	Z1					✓	✓	✓		✓			
Marti et al. (1995)	A, glass					✓	✓			✓		✓	✓
	B, glass					✓	✓			✓		✓	✓
	Normal					✓	✓			✓		✓	✓
Eugster et al. (1996); Eugster et al. (1997)	BE-532	✓	✓	✓	✓	✓	✓						
Grady et al. (1997)	Whole-rock, BM 1966,54											✓	✓
	Whole-rock, BM 1966,54											✓	✓
	Fine lithology, UNM A23,9											✓	✓
	Coarse lithology, UNM A23,12d											✓	✓
	Glass (fine), UNM A23,9											✓	✓
	Glass (coarse) UNM A23,12d											✓	✓
	Pigeonite (coarse), A23,12de											✓	✓
Mathew et al. (1998)	,1 dark lithol.									✓	✓	✓	✓

Table A2. Results for He and Ne. He concentrations in 10^{-8}, Ne concentrations in 10^{-9} cc STP/g.

Sample	Temperature (°C)	^{4}He	^{3}He/^{4}He	^{22}Ne	^{20}Ne/^{22}Ne	^{21}Ne/^{22}Ne
Shergotty whole rock (40.3 mg)	800	121 ± 1	0.0315 ± 0.0013	3.18 ± 0.24	0.866 ± 0.029	0.803 ± 0.007
	1800	0.174 ± 0.016	0.0258 ± 0.0167	3.80 ± 0.29	0.866 ± 0.009	0.755 ± 0.014
	Sum	121 ± 1	0.0315 ± 0.0013	6.98 ± 0.37	0.866 ± 0.014	0.777 ± 0.008
Shergotty pyroxene (123.12 mg)	400	1.78 ± 0.03	0.0097 ± 0.0005	–[a]	–[a]	–[a]
	800	113.25 ± 1.00	0.0347 ± 0.0011	1.09 ± 0.01	0.906 ± 0.008	0.805 ± 0.008
	1200	5.62 ± 0.05	0.0080 ± 0.0002	2.60 ± 0.14	0.829 ± 0.007	0.821 ± 0.009
	1500	3.00 ± 0.16	0.0003 ± 0.0001	3.29 ± 0.18	0.834 ± 0.006	0.826 ± 0.008

Table A2. *Continued.* Results for He and Ne. He concentrations in 10^{-8}, Ne concentrations in 10^{-9} cc STP/g.

Sample	Temperature (°C)	^{4}He	^{3}He/^{4}He	^{22}Ne	^{20}Ne/^{22}Ne	^{21}Ne/^{22}Ne
	1700	2.73 ± 0.03	–[a]	–[a]	–[a]	–[a]
	Sum	126.38 ± 1.01	0.0316 ± 0.0009	6.98 ± 0.23	0.843 ± 0.004	0.821 ± 0.005
Shergotty maskelynite (39 mg)	350	2.36 ± 0.03	0.0381 ± 0.0010	0.16 ± 0.01	2.74 ± 0.06	0.587 ± 0.009
	988	94.3 ± 0.9	0.00882 ± 0.00022	7.90 ± 0.42	0.729 ± 0.007	0.734 ± 0.008
	1535	0.186 ± 0.016	0.00286 ± 0.00261	0.44 ± 0.02	0.853 ± 0.023	0.825 ± 0.010
	1535	–[a]	–[a]	–[a]	–[a]	–[a]
	Sum	96.9 ± 0.9	0.00952 ± 0.00021	8.50 ± 0.42	0.773 ± 0.007	0.736 ± 0.007
Zagami whole rock (51.4 mg)	800	272 ± 19	0.0174 ± 0.0003	3.57 ± 0.26	0.859 ± 0.020	0.844 ± 0.004
	1800	2.0 ± 1.2	0.0052 ± 0.0003	3.39 ± 0.25	0.841 ± 0.005	0.788 ± 0.003
	1900	–[a]	–[a]	–[a]	–[a]	–[a]
	Sum	274 ± 19	0.0173 ± 0.0003	6.96 ± 0.36	0.850 ± 0.011	0.817 ± 0.004
Zagami pyroxene (46.9 mg)	400	5.1 ± 1.8	0.0916 ± 0.0060	0.0489 ± 0.0040	2.006 ± 0.221	0.669 ± 0.031
	800	151 ± 2	0.0278 ± 0.0005	0.814 ± 0.054	0.879 ± 0.021	0.802 ± 0.032
	1200	1.40 ± 1.4	0.0315 ± 0.0011	3.82 ± 0.26	0.825 ± 0.007	0.823 ± 0.033
	1550	–[a]	–[a]	1.51 ± 0.10	0.849 ± 0.015	0.819 ± 0.033
	1600	–[a]	–[a]	–[a]	–[a]	–[a]
	Sum	158 ± 3	0.0299 ± 0.0009	6.20 ± 0.28	0.847 ± 0.007	0.818 ± 0.022
Zagami maskelynite (14 mg)	400	14.2 ± 6.1	0.0123 ± 0.0008	0.447 ± 0.031	1.048 ± 0.108	0.657 ± 0.027
	800	48.4 ± 6.1	0.0159 ± 0.0009	8.11 ± 0.55	0.681 ± 0.008	0.697 ± 0.028
	1200	–[a]	–[a]	0.807 ± 0.055	0.772 ± 0.062	0.810 ± 0.033
	1600	–[a]	–[a]	0.062 ± 0.009	2.191 ± 0.454	0.710 ± 0.050
	1600	–[a]	–[a]	–[a]	–[a]	–[a]
	Sum	62.6 ± 8.6	0.0151 ± 0.0008	9.426 ± 0.554	0.716 ± 0.011	0.705 ± 0.024
EETA79001 whole rock (48.7 mg)	800	32.0 ± 3.5	0.0301 ± 0.0017	0.741 ± 0.055	0.811 ± 0.023	0.743 ± 0.004
	1800	1.4 ± 1.3	0.0074 ± 0.0004	1.108 ± 0.082	0.883 ± 0.069	0.764 ± 0.006
	1900	–[a]	–[a]	–[a]	–[a]	–[a]
	Sum	33.4 ± 3.7	0.0291 ± 0.0017	1.849 ± 0.099	0.855 ± 0.043	0.755 ± 0.004
EETA79001 pyroxene (94.3 mg)	400	19.21 ± 0.18	0.0280 ± 0.0007	0.203 ± 0.004	0.790 ± 0.024	0.720 ± 0.009
	800	17.26 ± 0.14	0.0262 ± 0.0006	0.470 ± 0.008	0.831 ± 0.012	0.749 ± 0.008
	1000	0.24 ± 0.03	0.0444 ± 0.0060	0.274 ± 0.005	0.865 ± 0.020	0.761 ± 0.008
	1400	0.02 ± 0.01	0.0300 ± 0.0108	0.579 ± 0.010	0.857 ± 0.014	0.750 ± 0.009
	1650	–[a]	–[a]	0.005 ± 0.001	1.586 ± 1.038	0.712 ± 0.236
	1700	–[a]	–[a]	0.020 ± 0.001	1.545 ± 0.298	0.668 ± 0.054
	1780	–[a]	–[a]	–[a]	–[a]	–[a]
	Sum	36.72 ± 0.23	0.0273 ± 0.0005	1.551 ± 0.014	0.853 ± 0.009	0.746 ± 0.005

[a]Close to or below blank.

Table A3. Results for Ar. Concentrations are given in 10^{-9} cc STP/g.

Sample	Temperature (°C)	^{36}Ar	^{40}Ar	^{38}Ar/^{36}Ar	^{40}Ar/^{36}Ar
Shergotty whole rock (40.3 mg)	800	0.97 ± 0.09	1283 ± 105	0.508 ± 0.052	1318 ± 72
	1800	2.08 ± 0.09	969 ± 50	1.199 ± 0.053	466 ± 17
	Sum	3.05 ± 0.13	2253 ± 116	0.979 ± 0.041	738 ± 24
Shergotty pyroxene (123.12 mg)	400	–[a]	–[a]	–[a]	–[a]
	800	0.39 ± 0.02	713 ± 33	0.350 ± 0.006	1850 ± 57
	1200	0.40 ± 0.02	386 ± 18	0.839 ± 0.015	957 ± 29
	1500	1.96 ± 0.07	499 ± 23	1.344 ± 0.028	254 ± 7
	1700	0.09 ± 0.01	26 ± 4	0.933 ± 0.038	293 ± 28
	Sum	2.84 ± 0.08	1624 ± 44	1.125 ± 0.020	572 ± 13
Shergotty maskelynite (39 mg)	*350*	*0.08 ± 0.02*	*26 ± 11*	*0.198 ± 0.014*	*341 ± 100*
	988	1.06 ± 0.05	1862 ± 86	0.799 ± 0.016	1764 ± 56
	1535	1.91 ± 0.08	1871 ± 106	1.171 ± 0.019	979 ± 43
	1535	–[a]	–[a]	–[a]	–[a]
	Sum	2.97 ± 0.09	3733 ± 137	1.039 ± 0.014	1258 ± 34
Zagami whole rock (51.4 mg)	800	0.91 ± 0.05	1339 ± 52	0.615 ± 0.048	1476 ± 89
	1800	2.50 ± 0.05	762 ± 17	1.373 ± 0.022	305 ± 6
	1900	–[a]	–[a]	–[a]	–[a]
	Sum	3.41 ± 0.07	2102 ± 55	1.171 ± 0.022	617 ± 14
Zagami pyroxene (46.9 mg)	400	–[a]	–[a]	–[a]	–[a]
	800	0.19 ± 0.04	584 ± 23	0.542 ± 0.037	3060 ± 291
	1200	0.65 ± 0.04	283 ± 22	1.264 ± 0.055	436 ± 21
	1550	1.35 ± 0.05	109 ± 22	1.433 ± 0.035	80 ± 13
	1600	–[a]	–[a]	–[a]	–[a]
	Sum	2.19 ± 0.08	976 ± 38	1.306 ± 0.029	445 ± 43
Zagami maskelynite (14 mg)	400	–[a]	–[a]	–[a]	–[a]
	800	0.18 ± 0.14	486 ± 73	0.955 ± 0.098	2649 ± 388
	1200	1.35 ± 0.14	1554 ± 73	1.277 ± 0.078	1153 ± 64
	1600	0.78 ± 0.14	823 ± 73	1.238 ± 0.102	1060 ± 86
	1600	–[a]	–[a]	–[a]	–[a]
	Sum	2.31 ± 0.25	2863 ± 129	1.238 ± 0.057	1241 ± 56
EETA79001 whole rock (48.7 mg)	800	0.37 ± 0.02	464 ± 16	0.353 ± 0.028	1269 ± 62
	1800	0.49 ± 0.04	455 ± 18	0.951 ± 0.051	933 ± 49
	1900	–[a]	–[a]	–[a]	–[a]
	Sum	0.85 ± 0.04	919 ± 24	0.695 ± 0.032	1077 ± 39
EETA79001 pyroxene (94.3 mg)	*400*	*0.16 ± 0.01*	*65 ± 2*	*0.204 ± 0.010*	*398 ± 34*
	800	0.17 ± 0.01	241 ± 6	0.525 ± 0.020	1433 ± 121
	1000	0.05 ± 0.05	121 ± 15	1.592 ± 0.194	2221 ± 266
	1400	0.24 ± 0.05	163 ± 15	1.577 ± 0.155	666 ± 46
	1650	0.03 ± 0.05	9 ± 15	0.141 ± 0.096	290 ± 37

Table A3. *Continued.* Results for Ar. Concentrations are given in 10^{-9} cc STP/g.

Sample	Temperature (°C)	^{36}Ar	^{40}Ar	$^{38}Ar/^{36}Ar$	$^{40}Ar/^{36}Ar$
	1700	*0.10 ± 0.05*	*31 ± 15*	*0.195 ± 0.030*	*302 ± 13*
	1780	0.21 ± 0.05	64 ± 15	0.174 ± 0.015	299 ± 9
	Sum	0.46 ± 0.07	525 ± 23	1.199 ± 0.092	1124 ± 56

[a]Close to or below blank.

Data in italics have close to atmospheric isotopic ratios and are suspected to be dominated by air contamination and/or (at high extraction temperature) excessive blank. They are not included in the totals.

Table A4. Results for krypton. Concentrations in 10^{-12} cc STP/g.

Sample	Temperature (°C)	^{84}Kr	$^{78}Kr/^{84}Kr$	$^{80}Kr/^{84}Kr$	$^{82}Kr/^{84}Kr$	$^{83}Kr/^{84}Kr$	$^{86}Kr/^{84}Kr$
Shergotty whole rock (40.3 mg)	800	23.62 ± 1.82	0.0098 ± 0.0008	0.0495 ± 0.0019	0.2084 ± 0.0031	0.2153 ± 0.0035	0.3082 ± 0.0088
	1800	33.83 ± 2.60	0.0128 ± 0.0009	0.0595 ± 0.0020	0.2272 ± 0.0031	0.2325 ± 0.0035	0.2917 ± 0.0055
	Sum	57.46 ± 3.17	0.0116 ± 0.0006	0.0554 ± 0.0014	0.2194 ± 0.0022	0.2254 ± 0.0025	0.2985 ± 0.0049
Shergotty pyroxene (123.12 mg)	400	–[a]	–[a]	–[a]	–[a]	–[a]	–[a]
	800	7.12 ± 0.44	0.0015 ± 0.0173	0.0449 ± 0.0026	0.2041 ± 0.0066	0.2076 ± 0.0054	0.3000 ± 0.0071
	1200	6.39 ± 0.41	---	0.0651 ± 0.0033	0.2437 ± 0.0058	0.2289 ± 0.0087	0.2955 ± 0.0146
	1500	10.32 ± 0.53	0.0079 ± 0.0120	0.0574 ± 0.0007	0.2208 ± 0.0104	0.2276 ± 0.0038	0.3099 ± 0.0055
	1700	–[a]	–[a]	–[a]	–[a]	–[a]	–[a]
	Sum	23.83 ± 0.80	–	0.0557 ± 0.0012	0.2220 ± 0.0052	0.2220 ± 0.0033	0.3031 ± 0.0051
Shergotty maskelynite (39 mg)	350	1.92 ± 0.94	–[a]	0.0181 ± 0.0147	0.2129 ± 0.0285	0.1773 ± 0.0263	0.2163 ± 0.0526
	988	10.10 ± 1.04	–[a]	0.0621 ± 0.0059	0.2372 ± 0.0110	0.2784 ± 0.0136	0.2882 ± 0.0163
	1535	23.97 ± 1.39	0.0201 ± 0.0160	0.0995 ± 0.0048	0.2751 ± 0.0071	0.3014 ± 0.0071	0.2891 ± 0.0103
	1535	–[a]	–[a]	–[a]	–[a]	–[a]	–[a]
	Sum	34.07 ± 1.74	–	0.0884 ± 0.0039	0.2639 ± 0.0060	0.2946 ± 0.0064	0.2888 ± 0.0187
Zagami whole rock (51.4 mg)	800	26.26 ± 1.92	0.1251 ± 0.0027	0.0524 ± 0.0012	0.2310 ± 0.0066	0.2182 ± 0.0026	0.2941 ± 0.0042
	1800	34.53 ± 2.62	0.0143 ± 0.0009	0.0613 ± 0.0016	0.2258 ± 0.0024	0.2358 ± 0.0030	0.2928 ± 0.0047
	1900	–[a]	–[a]	–[a]	–[a]	–[a]	–[a]
	Sum	60.78 ± 3.25	0.0622 ± 0.0021	0.0575 ± 0.0011	0.2280 ± 0.0032	0.2281 ± 0.0020	0.2932 ± 0.0032
Zagami pyroxene (46.9 mg)	400	–[a]	–[a]	–[a]	–[a]	–[a]	–[a]
	800	3.05 ± 0.50	–[a]	0.0467 ± 0.0097	0.2027 ± 0.0189	0.2564 ± 0.1123	0.2798 ± 0.0189
	1200	5.59 ± 0.53	0.0125 ± 0.0343	0.0756 ± 0.0069	0.2657 ± 0.0139	0.2537 ± 0.0081	0.3164 ± 0.0167
	1550	3.76 ± 0.51	–[a]	0.0624 ± 0.0092	0.2358 ± 0.0206	0.2450 ± 0.0242	0.2830 ± 0.0111
	1600	1.45 ± 0.50	–[a]	0.0245 ± 0.0196	0.2144 ± 0.0127	0.2268 ± 0.0362	0.2863 ± 0.0224
	Sum	13.85 ± 1.02	–	0.0499 ± 0.0062	0.2222 ± 0.0097	0.2469 ± 0.0460	0.2872 ± 0.0097

Table A4. *Continued.* Results for krypton. Concentrations in 10^{-12} cc STP/g.

Sample	Temperature (°C)	^{84}Kr	^{78}Kr/^{84}Kr	^{80}Kr/^{84}Kr	^{82}Kr/^{84}Kr	^{83}Kr/^{84}Kr	^{86}Kr/^{84}Kr
Zagami maskelynite (14 mg)	400	–[a]	–[a]	–[a]	–[a]	–[a]	–[a]
	800	1.34 ± 1.65	0.2588 ± 0.4612	0.0617 ± 0.0664	0.2383 ± 0.0974	0.0083 ± 0.1137	–[a]
	1200	9.82 ± 1.67	0.3605 ± 0.0639	0.1196 ± 0.0168	0.2884 ± 0.0119	0.3546 ± 0.0261	0.1832 ± 0.0221
	1600	7.18 ± 1.71	0.0211 ± 0.0866	0.1359 ± 0.0134	0.3833 ± 0.0254	0.3662 ± 0.0285	0.3130 ± 0.0159
	1600	–[a]	–[a]	–[a]	–[a]	–[a]	–[a]
	Sum	18.34 ± 2.91	–	0.1217 ± 0.0122	0.3219 ± 0.0145	0.3338 ± 0.0314	0.2204 ± 0.0242
EETA79001 whole rock (48.7 mg)	800	14.51 ± 1.09	0.0060 ± 0.0009	0.0415 ± 0.0017	0.2069 ± 0.0032	0.2152 ± 0.0039	0.3048 ± 0.0079
	1800	21.91 ± 1.77	0.0020 ± 0.0012	0.0445 ± 0.0016	0.2169 ± 0.0066	0.2067 ± 0.0047	0.3005 ± 0.0048
	1900	*7.22 ± 1.03*	*0.0061 ± 0.0035*	*0.0385 ± 0.0045*	*0.2060 ± 0.0050*	*0.1964 ± 0.0105*	*0.3541 ± 0.0139*
	Sum	43.64 ± 2.32	0.0040 ± 0.0009	0.0425 ± 0.0013	0.2118 ± 0.0036	0.208 ± 0.003	0.3108 ± 0.0042
EETA79001 pyroxene (94.3 mg)	400	5.44 ± 0.31	0.0110 ± 0.0024	0.0399 ± 0.0013	0.1997 ± 0.0083	0.2024 ± 0.0033	0.3040 ± 0.0051
	800	1.93 ± 0.18	0.0235 ± 0.0071	0.0528 ± 0.0102	0.2194 ± 0.0149	0.1838 ± 0.0107	0.3333 ± 0.0233
	1000	1.91 ± 0.32	0.0279 ± 0.0097	0.0542 ± 0.0027	0.2258 ± 0.0094	0.2290 ± 0.0060	0.2800 ± 0.0096
	1400	5.19 ± 0.39	0.0044 ± 0.0044	0.0463 ± 0.0018	0.2120 ± 0.0035	0.2122 ± 0.0054	0.3204 ± 0.0147
	1650	1.75 ± 0.31	–[a]	0.0388 ± 0.0034	0.2019 ± 0.0051	0.2005 ± 0.0087	0.3268 ± 0.0088
	1700	1.56 ± 0.31	0.0357 ± 0.0112	0.0385 ± 0.0027	0.2058 ± 0.0070	0.1977 ± 0.0091	0.3745 ± 0.0342
	1780	*2.80 ± 0.33*	*–[a]*	*0.0398 ± 0.0026*	*0.1978 ± 0.0037*	*0.2073 ± 0.0031*	*0.3075 ± 0.0053*
	Sum	17.78 ± 0.76	0.0129 ± 0.0035	0.0445 ± 0.0014	0.2090 ± 0.0034	0.2055 ± 0.0026	0.3178 ± 0.0062

[a]Close to or below blank.

Data in italics have close to atmospheric isotopic ratios and are suspected to be dominated by air contamination and/or (at high extraction temperature) excessive blank. They are not included in the totals.

Table A5. Results for xenon. Concentrations in 10^{-12} cc STP/g.

Sample	Temperature (°C)	^{132}Xe	^{124}Xe/^{132}Xe	^{126}Xe/^{132}Xe	^{128}Xe/^{132}Xe	^{129}Xe/^{132}Xe	^{130}Xe/^{132}Xe	^{131}Xe/^{132}Xe	^{134}Xe/^{132}Xe	^{136}Xe/^{132}Xe
Shergotty whole rock (40.3 mg)	800	6.66 ± 0.60	0.0079 ± 0.0019	0.0059 ± 0.0007	0.0732 ± 0.0036	1.1463 ± 0.0334	0.1529 ± 0.0047	0.8335 ± 0.0200	0.3825 ± 0.0090	0.3461 ± 0.0170
	1800	8.72 ± 0.42	0.0114 ± 0.0030	0.0172 ± 0.0017	0.0859 ± 0.0032	1.1798 ± 0.0253	0.1618 ± 0.0057	0.8091 ± 0.0302	0.3856 ± 0.0120	0.3435 ± 0.0168
	Sum	15.37 ± 0.73	0.0099 ± 0.0019	0.0123 ± 0.0010	0.0804 ± 0.0024	1.1653 ± 0.0204	0.1579 ± 0.0038	0.8196 ± 0.0192	0.3843 ± 0.0078	0.3446 ± 0.0120
Shergotty pyroxene (123.12 mg)	400	–[a]	–[a]	–[a]	–[a]	–[a]	–[a]	–[a]	–[a]	–[a]
	800	1.08 ± 0.18	0.0034 ± 0.0015	0.0026 ± 0.0009	0.0645 ± 0.0099	1.0740 ± 0.0460	0.1544 ± 0.0126	0.8187 ± 0.0441	0.3897 ± 0.0181	0.3141 ± 0.0194
	1200	1.06 ± 0.18	0.0091 ± 0.0020	0.0107 ± 0.0037	0.1012 ± 0.0149	1.1248 ± 0.0271	0.1472 ± 0.0205	0.7776 ± 0.0413	0.3934 ± 0.0149	0.3367 ± 0.0257
	1500	1.41 ± 0.19	0.0150 ± 0.0016	0.0262 ± 0.0021	0.0979 ± 0.0180	1.2860 ± 0.0352	0.1669 ± 0.0151	0.8105 ± 0.0412	0.4088 ± 0.0040	0.3262 ± 0.0075
	1700	–[a]	–[a]	–[a]	–[a]	–[a]	–[a]	–[a]	–[a]	–[a]
	Sum	3.54 ± 0.32	0.0097 ± 0.0010	0.0144 ± 0.0015	0.0887 ± 0.0069	1.1734 ± 0.0216	0.1572 ± 0.0094	0.8032 ± 0.0245	0.3984 ± 0.0073	0.3257 ± 0.0101
Shergotty maskelynite (39 mg)	*350*	*0.42 ± 0.53*	*0.0001 ± 0.0138*	*–[a]*	*0.0636 ± 0.0250*	*0.9622 ± 0.1127*	*0.1364 ± 0.0281*	*0.8036 ± 0.0843*	*0.3470 ± 0.0339*	*0.1522 ± 0.0588*
	988	1.33 ± 0.54	0.0060 ± 0.0015	0.0149 ± 0.0028	0.0562 ± 0.0139	1.1374 ± 0.0639	0.1803 ± 0.0260	0.7390 ± 0.0530	0.3745 ± 0.1987	0.3506 ± 0.0252
	1535	3.17 ± 0.57	0.0446 ± 0.0059	0.0733 ± 0.0378	0.1403 ± 0.0113	1.4388 ± 0.0710	0.2026 ± 0.0991	0.9224 ± 0.0461	0.3971 ± 0.0247	0.3421 ± 0.0171
	1535	*0.45 ± 0.54*	*0.0057 ± 0.0055*	*–[a]*	*0.0814 ± 0.0343*	*1.1298 ± 0.1573*	*0.1404 ± 0.0370*	*0.6551 ± 0.0996*	*0.3315 ± 0.0715*	*0.2567 ± 0.0587*
	Sum	4.50 ± 0.79	0.0332 ±	0.0560 ± 0.0269	0.1154 ± 0.0105	1.3497 ± 0.0569	0.1960 ± 0.0703	0.8682 ± 0.0380	0.3904 ± 0.0613	0.3446 ± 0.0142

Table A5. *Continued.* Results for xenon. Concentrations in 10^{-12} cc STP/g.

Sample	Temperature (°C)	^{132}Xe	^{124}Xe/^{132}Xe	^{126}Xe/^{132}Xe	^{128}Xe/^{132}Xe	^{129}Xe/^{132}Xe	^{130}Xe/^{132}Xe	^{131}Xe/^{132}Xe	^{134}Xe/^{132}Xe	^{136}Xe/^{132}Xe
Zagami whole rock (51.4 mg)	800	9.05 ± 0.54	0.0043 ± 0.0006	0.0063 ± 0.0008	0.0753 ± 0.0021	1.0252 ± 0.0239	0.1643 ± 0.0036	0.8073 ± 0.0115	0.3834 ± 0.0092	0.3328 ± 0.0090
	1800	12.38 ± 0.47	0.0132 ± 0.0014	0.0175 ± 0.0012	0.0935 ± 0.0018	1.1090 ± 0.0177	0.1654 ± 0.0031	0.8062 ± 0.0076	0.3825 ± 0.0067	0.3223 ± 0.0039
	1900	2.68 ± 0.24	0.0024 ± 0.0055	0.0008 ± 0.0026	–[a]	0.8723 ± 0.0486	0.1444 ± 0.0070	0.7370 ± 0.0307	0.3817 ± 0.0192	0.3325 ± 0.0135
	Sum	21.43 ± 0.72	0.0094 ± 0.0009	0.0127 ± 0.0008	0.0858 ± 0.0014	1.0736 ± 0.0144	0.1649 ± 0.0024	0.8067 ± 0.0065	0.3829 ± 0.0056	0.3267 ± 0.0044
Zagami pyroxene (46.9 mg)	400	–[a]	–[a]	–[a]	–[a]	–[a]	–[a]	–[a]	–[a]	–[a]
	800	0.34 ± 0.19	0.0044 ± 0.0021	0.0036 ± 0.0025	0.0565 ± 0.0137	0.8859 ± 0.1273	0.1051 ± 0.0186	0.7876 ± 0.0541	0.3818 ± 0.0273	0.3143 ± 0.0809
	1200	1.12 ± 0.19	0.0213 ± 0.0024	0.0334 ± 0.0038	0.1109 ± 0.0062	1.1667 ± 0.0288	0.1820 ± 0.0072	0.7711 ± 0.0404	0.3779 ± 0.0222	0.3247 ± 0.0421
	1550	0.65 ± 0.19	0.0120 ± 0.0037	0.0346 ± 0.0049	0.0977 ± 0.0168	1.1008 ± 0.0674	0.1884 ± 0.0210	0.7890 ± 0.1112	0.3863 ± 0.0617	0.2964 ± 0.0652
	1600	–[a]	–[a]	–[a]	–[a]	–[a]	–[a]	–[a]	–[a]	–[a]
	Sum	2.11 ± 0.33	0.0157 ± 0.0020	0.0290 ± 0.0030	0.0981 ± 0.0072	1.1013 ± 0.0362	0.1716 ± 0.0092	0.7793 ± 0.0414	0.3811 ± 0.0228	0.3143 ± 0.0328
Zagami maskelynite (14 mg)	400	–[a]	–[a]	–[a]	–[a]	–[a]	–[a]	–[a]	–[a]	–[a]
	800	0.11 ± 0.62	0.0273 ± 0.0146	0.0341 ± 0.0165	–[a]	1.9299 ± 0.6814	–[a]	0.7663 ± 0.4349	0.4743 ± 0.2255	0.5468 ± 0.2845
	1200	0.91 ± 0.62	0.0411 ± 0.0082	0.0820 ± 0.0157	0.1311 ± 0.2624	1.4246 ± 0.1418	0.2217 ± 0.0619	0.8450 ± 0.0767	0.4672 ± 0.0640	0.2502 ± 0.0995
	1600	0.48 ± 0.62	0.1176 ± 0.0276	0.1218 ± 0.0230	0.3181 ± 0.0567	1.5252 ± 0.1529	0.4320 ± 0.0872	1.3880 ± 0.1936	0.3389 ± 0.0552	0.2558 ± 0.0448
	1600	–[a]	–[a]	–[a]	–[a]	–[a]	–[a]	–[a]	–[a]	–[a]
	Sum	1.50 ± 1.07	0.0646 ± 0.0140	0.1954 ± 0.1745	0.2021 ± 0.0716	1.4934 ± 0.2009	0.2941 ± 0.0559	1.0119 ± 0.1061	0.4267 ± 0.0458	0.2744 ± 0.1177
EETA79001 whole rock (48.7 mg)	800	4.20 ± 0.48	0.0028 ± 0.0010	0.0038 ± 0.0027	0.0688 ± 0.0041	1.0129 ± 0.0345	0.1513 ± 0.0073	0.7642 ± 0.0172	0.3777 ± 0.0107	0.3168 ± 0.0128
	1800	6.26 ± 0.31	0.0034 ± 0.0025	0.0039 ± 0.0015	0.0697 ± 0.0031	1.1690 ± 0.0280	0.1491 ± 0.0049	0.7984 ± 0.0090	0.3892 ± 0.0110	0.3370 ± 0.0073
	1900	3.15 ± 0.25	0.0022 ± 0.0050	0.0043 ± 0.0026	0.0665 ± 0.0032	0.9146 ± 0.0457	0.1712 ± 0.0180	0.7566 ± 0.0149	0.3624 ± 0.0162	0.3153 ± 0.0089
	Sum	10.46 ± 0.57	0.0032 ± 0.0015	0.0039 ± 0.0014	0.0693 ± 0.0025	1.1063 ± 0.0219	0.1500 ± 0.0041	0.7847 ± 0.0088	0.3846 ± 0.0079	0.3289 ± 0.0068
EETA79001 pyroxene (94.3 mg)	*400*	*2.14 ± 0.08*	*0.0034 ± 0.0004*	*0.0033 ± 0.0010*	*0.0705 ± 0.0032*	*0.9821 ± 0.0162*	*0.1540 ± 0.0035*	*0.8088 ± 0.0052*	*0.3844 ± 0.0069*	*0.3264 ± 0.0046*
	800	1.32 ± 0.03	0.0038 ± 0.0004	0.0032 ± 0.0006	0.0735 ± 0.0039	1.0158 ± 0.0220	0.1499 ± 0.0043	0.7204 ± 0.0181	0.3822 ± 0.0058	0.3138 ± 0.0104
	1000	0.38 ± 0.12	0.0049 ± 0.0042	0.0105 ± 0.0016	0.0915 ± 0.0144	1.3347 ± 0.0864	0.1607 ± 0.0220	0.7946 ± 0.0486	0.3953 ± 0.0172	0.3854 ± 0.0465
	1400	1.24 ± 0.13	0.0047 ± 0.0062	0.0046 ± 0.0009	0.0874 ± 0.0113	1.2063 ± 0.0289	0.1576 ± 0.0079	0.8020 ± 0.0199	0.3609 ± 0.0153	0.3478 ± 0.0127
	1650	0.71 ± 0.12	0.0033 ± 0.0009	0.0038 ± 0.0010	0.0707 ± 0.0068	0.9568 ± 0.0154	0.1563 ± 0.0139	0.7911 ± 0.0303	0.3950 ± 0.0146	0.3065 ± 0.0194
	1700	0.36 ± 0.12	0.0033 ± 0.0014	0.0031 ± 0.0017	0.0604 ± 0.0136	1.1204 ± 0.0353	0.1354 ± 0.0203	0.8446 ± 0.0624	0.2987 ± 0.0416	0.3402 ± 0.0434
	1780	0.44 ± 0.12	0.0041 ± 0.0009	0.0032 ± 0.0014	0.0662 ± 0.0094	0.9803 ± 0.0301	0.1447 ± 0.0167	0.7958 ± 0.0722	0.3874 ± 0.0160	0.2991 ± 0.0323
	Sum	4.00 ± 0.25	0.0040 ± 0.0020	0.0044 ± 0.0004	0.0778 ± 0.0043	1.1035 ± 0.0149	0.1531 ± 0.0047	0.7763 ± 0.0125	0.3716 ± 0.0073	0.3322 ± 0.0086

[a]Close to or below blank.

Data in italics have close to atmospheric isotopic ratios and are suspected to be dominated by air contamination and/or (at high extraction temperature) excessive blank. They are not included in the totals.